NAVAL POSTGRADUATE SCHOOL

MONTEREY, CALIFORNIA

THESIS

FILTER BANK APPROACH TO THE ESTIMATION OF FLEXIBLE MODES IN DYNAMIC SYSTEMS

by

Konstantinos Tzellos

June 2007

Thesis Advisor: Roberto Cristi
Second Reader: Xiaoping Yun

Approved for public release; distribution is unlimited

THIS PAGE INTENTIONALLY LEFT BLANK

REPORT DOCUMENTATION PAGE			Form Approved OMB No. 0704-0188
Public reporting burden for this collection of information is estimated to average 1 hour per response, including the time for reviewing instruction, searching existing data sources, gathering and maintaining the data needed, and completing and reviewing the collection of information. Send comments regarding this burden estimate or any other aspect of this collection of information, including suggestions for reducing this burden, to Washington headquarters Services, Directorate for Information Operations and Reports, 1215 Jefferson Davis Highway, Suite 1204, Arlington, VA 22202-4302, and to the Office of Management and Budget, Paperwork Reduction Project (0704-0188) Washington DC 20503.			
1. AGENCY USE ONLY ***(Leave blank)***	**2. REPORT DATE** June 2007	**3. REPORT TYPE AND DATES COVERED** Master's Thesis	
4. TITLE AND SUBTITLE: Filter Bank Approach to the Estimation of Flexible Modes in Dynamic Systems			**5. FUNDING NUMBERS**
6. AUTHOR(S) Konstantinos Tzellos			
7. PERFORMING ORGANIZATION NAME(S) AND ADDRESS(ES) Naval Postgraduate School Monterey, CA 93943-5000			**8. PERFORMING ORGANIZATION REPORT NUMBER**
9. SPONSORING /MONITORING AGENCY NAME(S) AND ADDRESS(ES) N/A			**10. SPONSORING/MONITORING AGENCY REPORT NUMBER**
11. SUPPLEMENTARY NOTES The views expressed in this thesis are those of the author and do not reflect the official policy or position of the Department of Defense or the U.S. Government.			
12a. DISTRIBUTION / AVAILABILITY STATEMENT Approved for public release; distribution is unlimited			**12b. DISTRIBUTION CODE**

13. ABSTRACT (maximum 200 words)

The problem of estimating frequencies of sinusoids buried in noise has been of great interest in both military and civilian applications. In particular, in Control Systems with flexible appendages the sinusoidal vibrations can cause instabilities and degrade the performance of the overall system. In this thesis the problem of identifying frequencies of disturbances in flexible systems using advanced Digital Signal Processing techniques such as filter banks and Quadrature Mirror Filters is addressed. In a number of situations there is a need to design a controller for a system with flexible modes. In particular, in space applications solar panels and robotic arms introduce flexible modes in the system which degrades the performance. In these kinds of applications, the frequencies of the flexible modes can not be modeled accurately a priori and they can change according to the operating conditions. The proposed approach is tested by computer simulations.

14. SUBJECT TERMS Frequency Estimation, Filter Banks, Daubechies Filters, Discrete Fourier Transform, Finite Impulse Response, Flexible Structure Space, Highpass Filter, Inverse Discrete Fourier Transform, Lowpass Filter, Proportional Integral Derivative, Quadrature Mirror Filter, Signal-to-Noise Ratio, Wide Sense Stationary			**15. NUMBER OF PAGES** 75
			16. PRICE CODE
17. SECURITY CLASSIFICATION OF REPORT Unclassified	**18. SECURITY CLASSIFICATION OF THIS PAGE** Unclassified	**19. SECURITY CLASSIFICATION OF ABSTRACT** Unclassified	**20. LIMITATION OF ABSTRACT** UL

NSN 7540-01-280-5500 Standard Form 298 (Rev. 2-89)
Prescribed by ANSI Std. 239-18

THIS PAGE INTENTIONALLY LEFT BLANK

Approved for public release; distribution is unlimited

FILTER BANK APPROACH TO THE ESTIMATION OF FLEXIBLE MODES IN DYNAMIC SYSTEMS

Konstantinos Tzellos
Lieutenant Junior Grade, Hellenic Navy
B.S., Hellenic Naval Academy, 2000

Submitted in partial fulfillment of the
requirements for the degrees of

MASTER OF SCIENCE IN ELECTRICAL ENGINEERING

from the

NAVAL POSTGRADUATE SCHOOL
June 2007

Author: Konstantinos Tzellos

Approved by: Roberto Cristi
Thesis Advisor

Xiaoping Yun
Second Reader

Jeffrey B. Knorr
Chairman, Department of Electrical and Computer Engineering

THIS PAGE INTENTIONALLY LEFT BLANK

ABSTRACT

The problem of estimating frequencies of sinusoids buried in noise has been of great interest in both military and civilian applications. In particular, in Control Systems with flexible appendages the sinusoidal vibrations can cause instabilities and degrade the performance of the overall system. In this thesis the problem of identifying frequencies of disturbances in flexible systems using advanced Digital Signal Processing techniques such as filter banks and Quadrature Mirror Filters is addressed. In a number of situations there is a need to design a controller for a system with flexible modes. In particular, in space applications solar panels and robotic arms introduce flexible modes in the system which degrades the performance. In these kinds of applications, the frequencies of the flexible modes can not be modeled accurately a priori and they can change according to the operating conditions. The proposed approach is tested by computer simulations.

THIS PAGE INTENTIONALLY LEFT BLANK

TABLE OF CONTENTS

THIS PAGE INTENTIONALLY LEFT BLANK

LIST OF FIGURES

LIST OF TABLES

THIS PAGE INTENTIONALLY LEFT BLANK

LIST OF ABBREVIATIONS

dBN	Daubechies filter of order N
DFT	Discrete Fourier Transform
FB	Filter Bank
FIR	Finite Impulse Response
FSS	Flexible Structure Space
HPF	Highpass Filter
IDFT	Inverse Discrete Fourier Transform
LPF	Lowpass Filter
PID	Proportional Integral Derivative
QMF	Quadrature Mirror Filter
SNR	Signal-to-Noise Ratio
WSS	Wide Sense Stationary

THIS PAGE INTENTIONALLY LEFT BLANK

EXECUTIVE SUMMARY

Satellite systems are being deployed on a regular basis these days with various missions, namely civilian or military. Among them, at a great percentage, are communications and observation. However, it has been observed that for these cases the existing vibrations from the flexible surfaces of the satellite and the atmospheric interferences add colored noise and consequently undermine the system's performance. In this thesis an approach to estimate frequencies in noise based on Filter Banks and Quadrature Mirror Filters is developed. The general idea is to decompose the signal into components at various frequency bands and compute the relative energy in the single bands.

The Quadrature Mirror Filters approach is based on the Daubechies filters which guarantee orthogonality of the frequency components. The advantage of this approach is that it can be suitable for a non-uniform decomposition of the frequency axis, so that one can have a higher frequency resolution at desired parts of the spectrum.

The Discrete Fourier Transform (DFT) Filter Bank approach is based on an efficient bank of passband filters all derived by modulation of a prototype lowpass filter. In this case, orthogonality of the various frequency components can be guaranteed only by the use of ideal filters, which clearly cannot be achieved in practice. This can be approximated using a Finite Impulse Response (FIR) prototype lowpass filter with sufficient attenuation in the stopband. The technique is applied to the particular case of estimating the underdamped frequencies in flexible structures. For the Quadrature Mirror Filter case a recursive structure is devised, which provides recursive decomposition after frequency bands with higher energy.

THIS PAGE INTENTIONALLY LEFT BLANK

I. BACKGROUND THEORY / LITERATURE REVIEW

This chapter covers the theory of the DFT Filter Banks and the maximally decimated DFT Filter Banks used in this thesis. Furthermore, the Quadrature Mirror Filters, Daubechies filters, and ideal FIR Filters, which constitute the theoretical basis for this research, are covered as well.

A. DFT FILTER BANKS / TRANSMULTIPLEXERS

1. Introduction

In several applications, in order to be able to estimate the frequencies of sinusoids hidden in noise, there is a need to decompose the original signal into its subcomponents. This process, called "analysis," is the first part in the signal decomposition with "filter banks." The other part, called "synthesis," is the assembling of the decomposed signal again into one signal. The exactly reversed procedure is performed by the "transmultiplexers" and will be addressed later on. Based on [Cristi1], the diagrams in Figures 1 and 2 show the general case for both filter banks and transmultiplexers.

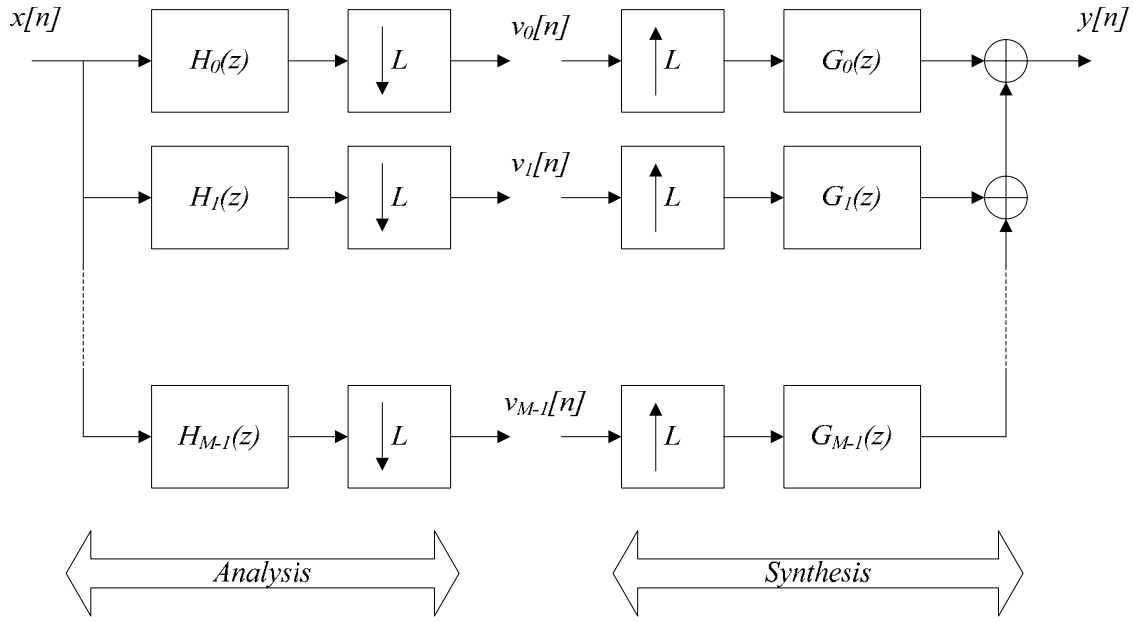

Figure 1. Filter Bank [After: Cristi1]

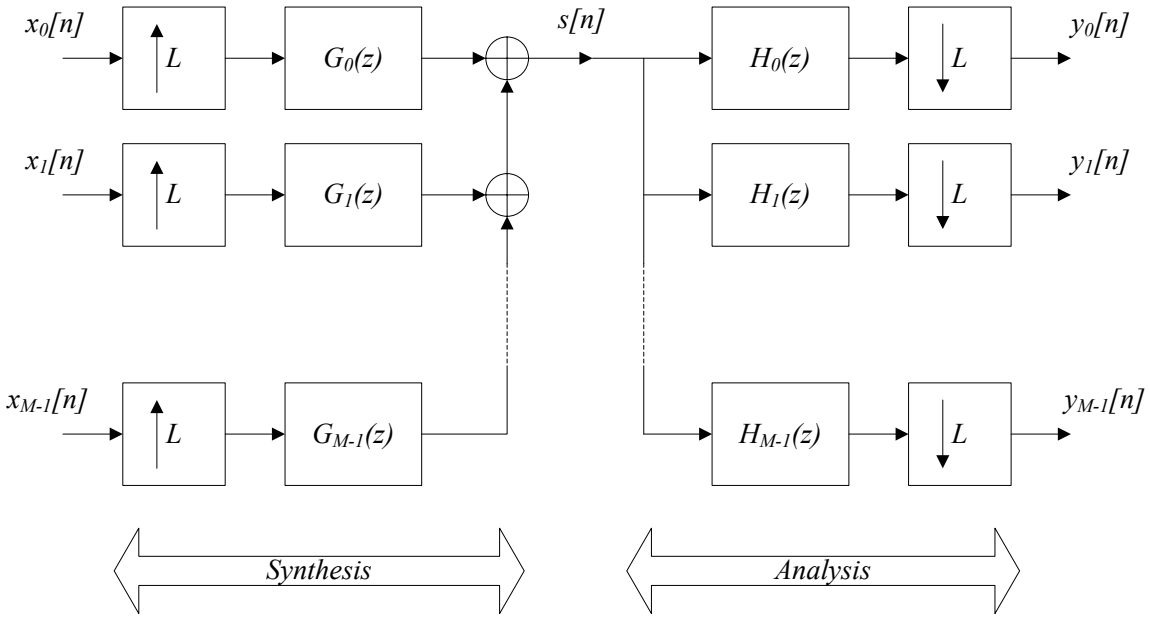

Figure 2. Transmultiplexer [After: Cristi1]

The benefit of using Filter Banks for frequency estimation is twofold. First, with the frequency decomposition it can be determined which of the narrower frequency bands contains the higher energy. Second, the data used for frequency estimation has better noise characteristics in terms of signal-to-noise ratio (SNR) and the noise is more "white."

2. DFT Filter Banks

The latter property is particularly attractive when one wants to estimate the frequency using a model-based approach. For the design of the filter bank, a prototype lowpass filter $H(\omega)$ with bandwidth π / M is used and from that, all the other filters are derived by shifting the filter in the frequency domain as given by

$$H_k(\omega) = H(\omega - k\frac{2\pi}{M}) \tag{1.1}$$

for $k=0,\ldots,M-1$ as shown in Figure 3. By doing so, no spectrum areas are left uncovered and the bandwidth is not exceeded.

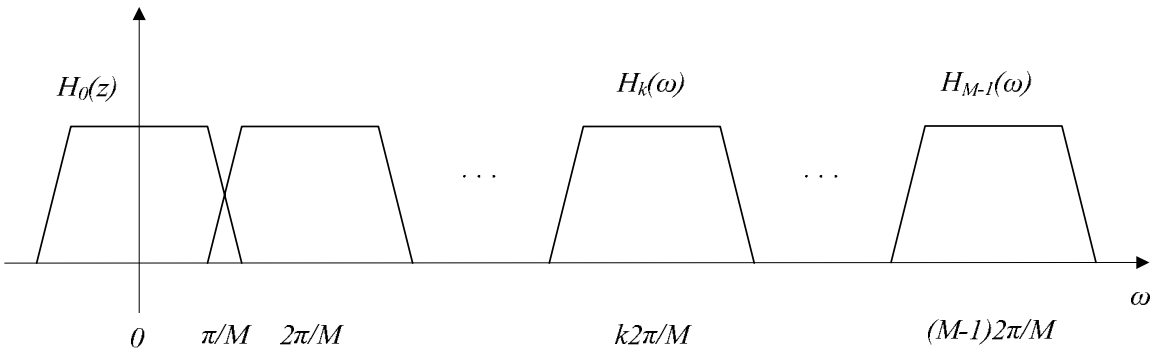

Figure 3. Frequency Spectrum Coverage [After: Cristi1]

It is easy to see that the transfer function of these filters can be written as

$$H_k(z) = H(e^{-j(k2\pi/M)}z),\ k=0,...,M-1 \tag{1.2}$$

If *H(z)* is decomposed into its noncausal polyphase components as

$$H(z) = \sum_{l=0}^{M-1} z^l E_{-l}(z^M),\ l=0,...,M-1 \tag{1.3}$$

Equation 1.1 becomes

$$\begin{aligned} H_k(z) = H(e^{-j(k2\pi/M)}z) = \sum_{l=0}^{M-1}(e^{-j(k2\pi/M)}z)^l E_{-l}((e^{-j(k2\pi/M)}z)^M) = \\ = \sum_{l=0}^{M-1} z^l e^{-j(kl2\pi/M)} E_{-l}(z^M e^{-j(k2\pi M/M)}) = \sum_{l=0}^{M-1} z^l e^{-j(kl2\pi/M)} E_{-l}(z^M) \end{aligned} \tag{1.4}$$

since $e^{-j(k2\pi M/M)} = 1$ for all integer *k*.

If the aforementioned equation is applied for *k=0*, then

$$H_0(z) = E_0(z^M) + zE_{-1}(z^M) + z^2E_{-2}(z^M) + ... + z^{M-1}E_{M-1}(z^M) \tag{1.5}$$

which can be written in matrix form as

$$H_k(z) = \begin{bmatrix} 1 & 1 & ... & 1 \end{bmatrix} \begin{bmatrix} E_0(z^M) \\ zE_{-1}(z^M) \\ \vdots \\ z^{M-1}E_{-M+1}(z^M) \end{bmatrix} \tag{1.6}$$

Similarly, the general form of Equation 1.4 can be written in a matrix form as

$$H_k(z) = \begin{bmatrix} 1 & e^{-j(k2\pi/M)} & \dots & e^{-j(k2\pi(M-1)/M)} \end{bmatrix} \begin{bmatrix} E_0(z^M) \\ zE_{-1}(z^M) \\ \vdots \\ z^{M-1}E_{-M+1}(z^M) \end{bmatrix} \tag{1.7}$$

Combining all M filters in one vector, the matrix becomes

$$\begin{bmatrix} H_0(z) \\ H_1(z) \\ \vdots \\ H_{M-1}(z) \end{bmatrix} = \begin{bmatrix} 1 & 1 & \cdots & 1 \\ 1 & e^{-j(k2\pi/M)} & \cdots & e^{-j(k2\pi(M-1)/M)} \\ \vdots & \vdots & \ddots & \vdots \\ 1 & e^{-j(k2\pi(M-1)/M)} & \cdots & e^{-j(k2\pi(M-1)^2/M)} \end{bmatrix} \begin{bmatrix} E_0(z^M) \\ zE_{-1}(z^M) \\ \vdots \\ z^{M-1}E_{-M+1}(z^M) \end{bmatrix} \tag{1.8}$$

By doing this, the analysis filter bank in Figure 1 is significantly simplified (less coefficients per filter) and can be implemented as in Figure 4, where E_k are the polyphase components of the prototype filter.

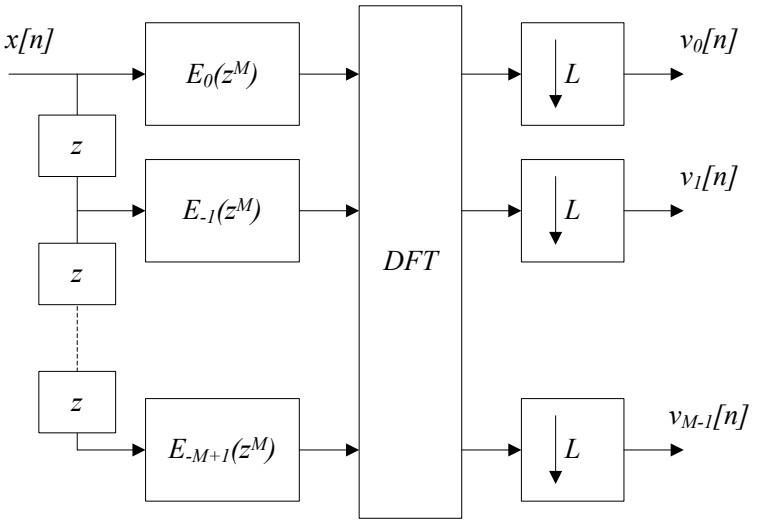

Figure 4. Filter Bank Analysis [From: Cristi1]

In this thesis, for the case of casual FIR filters, the formula that will be used for the polyphase decomposition is

$$H(z) = \sum_{l=0}^{M-1} z^{-l} E_l(z^M),\ l=0,\dots,M-1 \tag{1.9}$$

Due to the available block for unit delay in Simulink (z^{-1}), and by following the same procedure as before, the author gets the matrix below and the implementation of Figure 5.

$$\begin{bmatrix} H_0(z) \\ H_1(z) \\ \vdots \\ H_{M-1}(z) \end{bmatrix} = \begin{bmatrix} 1 & 1 & \cdots & 1 \\ 1 & e^{j(k2\pi/M)} & \cdots & e^{j(k2\pi(M-1)/M)} \\ \vdots & \vdots & \ddots & \vdots \\ 1 & e^{j(k2\pi(M-1)/M)} & \cdots & e^{j(k2\pi(M-1)^2/M)} \end{bmatrix} \begin{bmatrix} E_0(z^M) \\ z^{-1}E_1(z^M) \\ \vdots \\ z^{-M+1}E_{M-1}(z^M) \end{bmatrix} \quad (1.10)$$

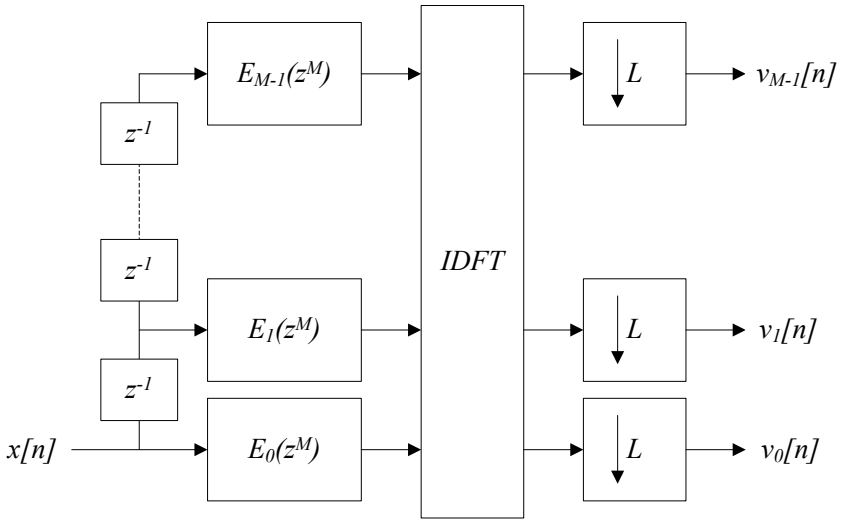

Figure 5. Thesis Filter Bank Implementation

3. Maximally Decimated DFT Filter Banks

The analysis filter bank is based on a number (bank) of bandpass filters with shifted frequency bands equally arranged to cover the whole spectrum. The maximally decimated case could be summarized as the decomposition of a signal x[n] into *M* channels $v_0[n]$, $v_1[n]$,…, $v_{M-1}[n]$, with each channel downsampled by *M*. Similarly, in the reverse process of synthesis, each of the *M* signals $v_0[n]$, $v_1[n]$,…, $v_{M-1}[n]$ are upsampled before being combined into the single signal y[n]. Figure 6 illustrates a network with a maximally decimated filter bank that is equivalent with the network in Figure 2, where *L=M*.

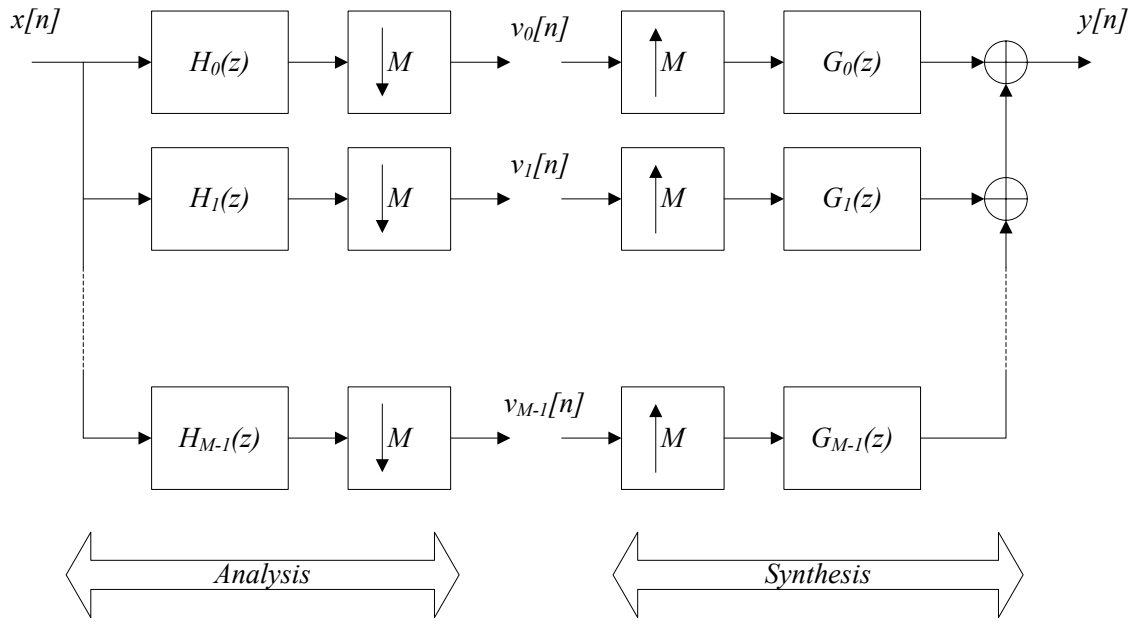

Figure 6. Maximally Decimated Filter Bank [From: Cristi1]

Based on the Noble Identity the above network can be reconstructed with the downsamplers repositioned and the z^M of the filters replaced as z. Figure 7 shows the implementation of the analysis and synthesis networks. Since the two operations of the DFT and the IDFT cancel each other out, the outcome is the equivalent system shown in Figure 8. Under certain conditions on the prototype filter, perfect reconstruction can be guaranteed.

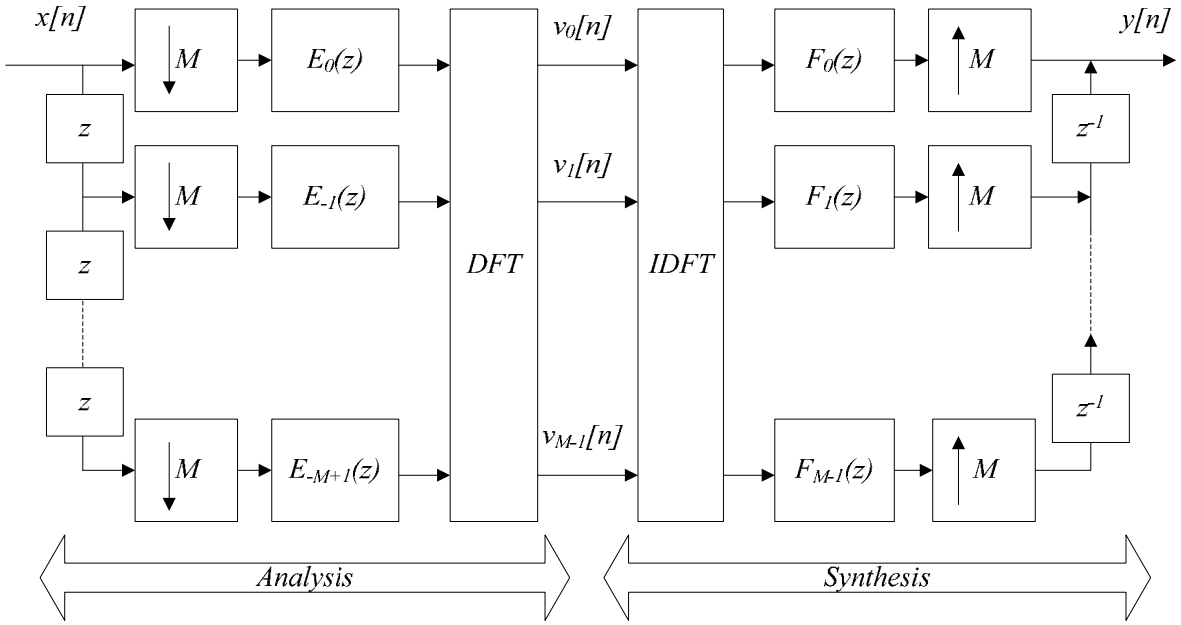

Figure 7. Maximally Decimated Analysis and Synthesis [After: Cristi1]

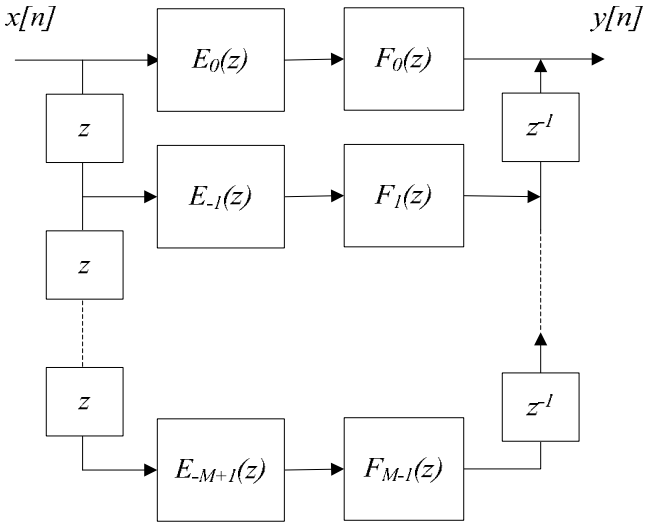

Figure 8. Equivalent Analysis and Synthesis

For the case of perfect reconstruction, the prototype filter *H(z)* used for the DFT analysis network and the prototype filter *G(z)* used for the DFT synthesis network must be such that

$$E_{-k}(z)F_k(z) = \frac{1}{M},\ k=0,\ldots,M-1 \tag{1.11}$$

From this condition it can be seen that if FIR filters are used, $E_{-k}(z)$ and $F_k(z)$ are simply zero degree polynomials (constant) and therefore considerably restrict the class of filters that can be used. In fact, it is easy to see that the only filters that can be used in the maximally decimated DFT filter banks are either ideal filters or FIR filters with length *M*. As a consequence, to guarantee perfect reconstruction, i.e., no loss of information, there is a need to downsample by a factor smaller than *M*. [Cristi], [Cristi1]

B. FIR FILTERS

The Ideal LP filter passes frequencies up to a cutoff frequency ω_c and rejects all frequencies above ω_c. In other words, its frequency response is

$$H_{LP}(e^{j\omega}) = \begin{cases} 1, & 0 \le \omega \le \omega_c \\ 0, & \omega_c < \omega \le \pi \end{cases} \tag{1.12}$$

Since its impulse response has an infinite length and it is non-causal this is non-realizable in practice. An approximation by an FIR filter can be parameterized by a passband ripple and stopband attenuation as shown in Figure 9.

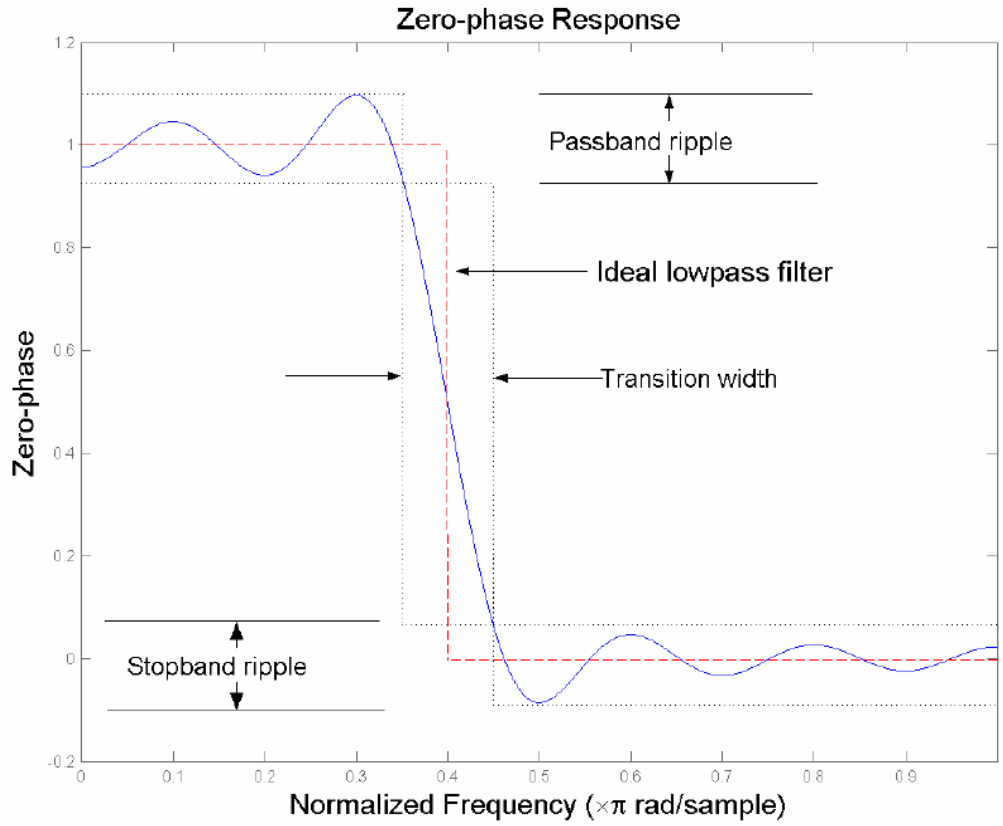

Figure 9. Example of Approximation of an Ideal FIR Filter [From: Losada]

Finally, it can be shown that the larger the order of the filter, the smaller the transition width and the ripples will be. So, depending on the application the filters are wanted for, the decision has to be made as to how "ideal" one wants them to be by selecting the allowed values for the transition region as well as the passband and stopband ripples.

C. QUADRATURE MIRROR FILTERS

Quadrature Mirror Filters are extensively used in subband coding of speech signal, image compression, communication systems, etc. With these filters, an input signal can be decomposed into its subband components and then resynthesized by them, with minor or no losses.

In the QMF approach, a signal is decomposed into two frequency bands, namely below and above $f_s/4$, *with* f_s being the sampling frequency. In addition, both signal

components are downsampled by two, thus keeping the same data rate. This is shown in the analysis network in Figure 10. In the synthesis section the signal is reconstructed, ideally without losses or distortion. Since the downsampling operation causes aliasing, particular care has to be taken in designing the two pairs of lowpass filter (LPF) and highpass filter (HPF).

By doing so, one gets two half-sampled signals at half the initial bandwidth each. Both signals are now downsampled by two so every other sample is dropped. Finally, for the analysis stage one gets the signal $y_1(n)$, which corresponds to the output of the lowpass filter and the signal $y_2(n)$, which corresponds to the highpass filter output. Again, the above procedure can be seen in Figure 10 below.

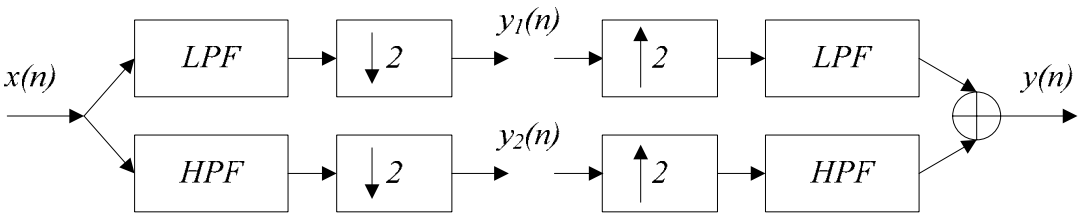

Figure 10. Two Subband QMF Analysis-Synthesis Scheme

It can be shown that one of the conditions for perfect reconstruction is that the sum of the Fourier transforms $H_L(e^{j\omega})$ and $H_H(e^{j\omega})$ of $h_L(n)$ and $h_H(n)$, respectively, must be at every frequency equal to one. [Jain]

$$\left|H_L\left(e^{j\omega}\right)\right|^2 + \left|H_H\left(e^{j\omega}\right)\right|^2 = 1 \qquad (1.13)$$

Figure 11 shows the highpass response magnitude as the mirror image of the lowpass response magnitude with respect to the middle frequency $\frac{\pi}{2}$ (Quadrature frequency).

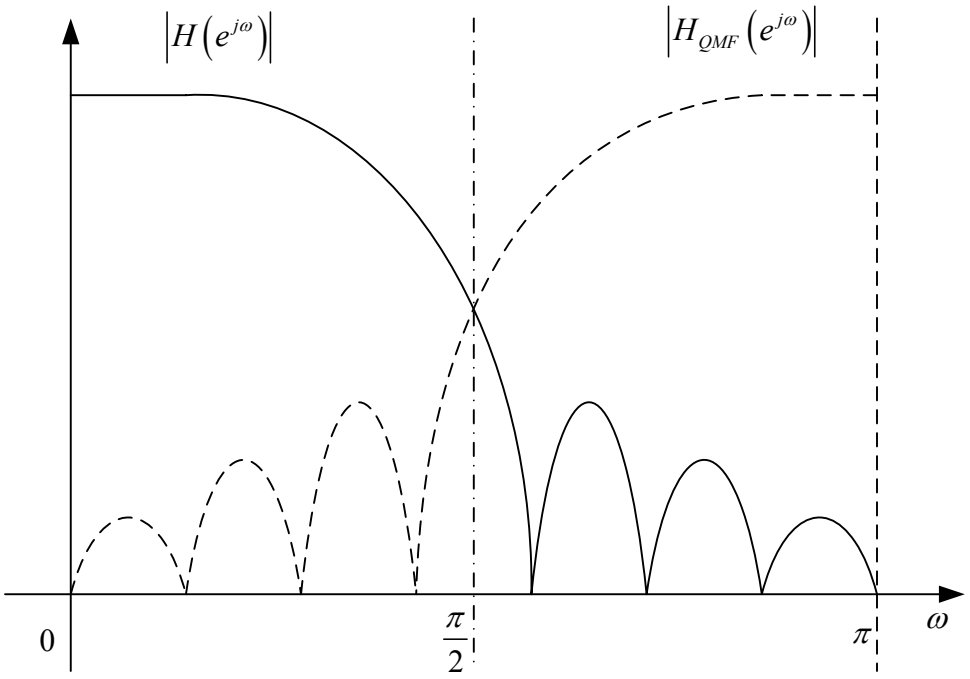

Figure 11. Quadrature Frequencies

One of the characteristics of this decomposition is that it preserves the energy of the signals, in the sense that

$$\sum_k \left|y_1[k]\right|^2 + \sum_k \left|y_2[k]\right|^2 = \sum_n \left|x[n]\right|^2 \tag{1.14}$$

with y_1, y_2 as the low frequency and high frequency components. Since this decomposition will be performed recursively in all components, the overall energy will be preserved throughout the overall decomposition. Likewise, if the same signal x is decomposed into N components $y_1, y_2, \ldots, y_N$, the above formula can be expanded as

$$\sum_{i=1}^{N} \sum_k \left|y_i[k]\right|^2 = \sum_n \left|x[n]\right|^2 \tag{1.15}$$

The reconstruction process is very similar to the decomposition. It is very easy to show that from the two outputs $y_1(n)$ and $y2(n)$, one can reconstruct a signal $x'(n)$ in a way that theoretically is identical to the original signal $x(n)$. The summary of the reconstruction is the two subband signals are interpolated by a factor of two and then after filtering them with another pair of filters, similarly made as in the analysis, the final signal $x'(n)$ is produced. [Swaminathan]

D. DAUBECHIES WAVELETS

For the implementation of the QMF bank a class of low complexity digital filters is used, namely the Daubechies family, that satisfy the property of the Quadrature Mirror Filters for energy preservation.

With the Daubechies filters included in Matlab's "Wavelet Toolbox," the perfect reconstruction condition is satisfied with FIR filters of low order. The command for these filters is "wfilters('dBN')," where N is related to the order. Each Daubechies filter generates a corresponding Daubechies Wavelet, shown in Figure 12. In this family of filters, for N=1 one has the simplest wavelet, the Haar Wavelet.

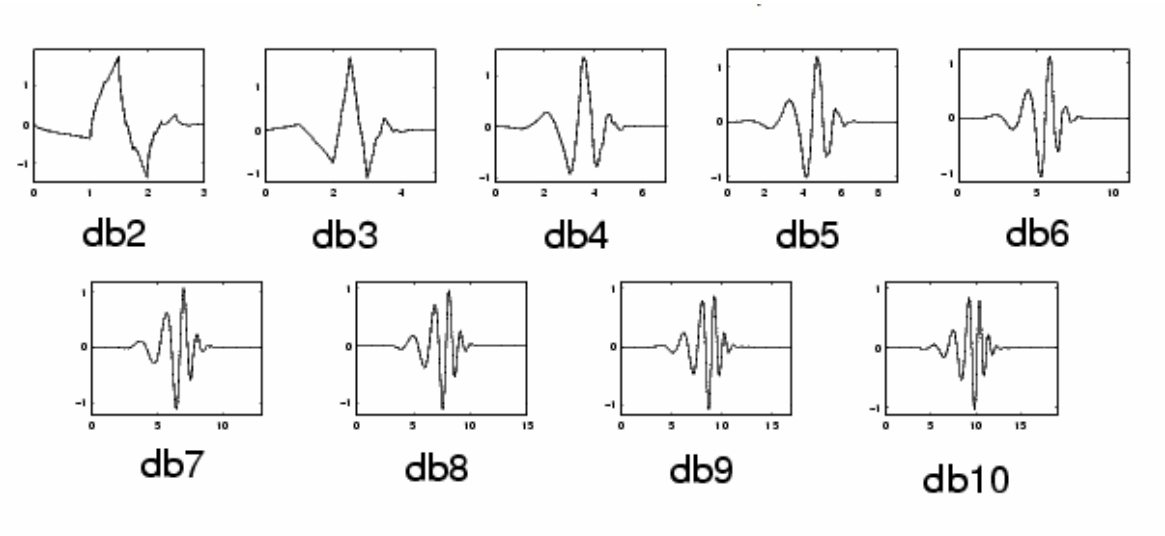

Figure 12. Examples of the Order of Daubechies Filters [From: Matlab]

If F_0 is a Daubechies scaling filter with $F_1=QMF(F_0)$ for its QMF, then the transfer functions of F_0 and F_1 will be according to Equation 1.12 [Matlab]:

$$\left|F_0(\omega)\right|^2+\left|F_1(\omega)\right|^2=1 \tag{1.16}$$

In order to visualize this, one can follow an example with "dB10" found in the Matlab's Wavelet Toolbox. On the first two plots in Figure 13, there is the lowpass filter for dB10 and its highpass Quadrature Mirror Filter. In the second row, the FFTs of the above filters, respectively, can be seen. Finally, in the last row there is the sum of the absolute values of the squared FFTs that are equal to one at each frequency, and thus proving that the QMF condition is satisfied [Matlab].

$$\left|\text{fft(filter)}\right|^2 + \left|\text{fft(qmf(filter))}\right|^2 = 1 \tag{1.17}$$

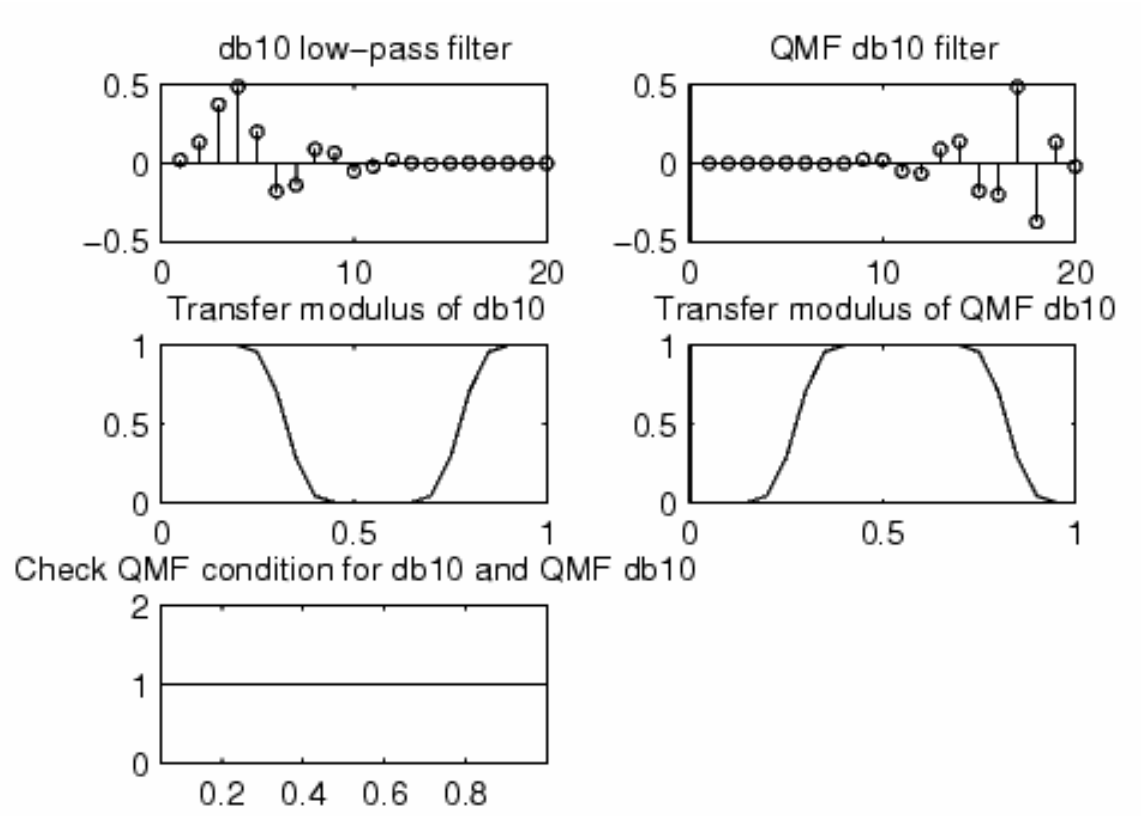

Figure 13. Example of the QMF Condition for the dB10 [From: Matlab]

E. THE FLATTENING OF NOISE IN THE SUBBANDS

1. Introduction

Below, it will be seen how the signal decomposition via the use of filter banks helps to better estimate the frequencies in the subbands than in the fullband by increasing the local SNR. The filters used are approximately ideal and there is minimal overlap between adjacent filters. It is well-known that parametric techniques to estimate signal models do not work well in the presence of colored noise. This is particularly true when this is applied to spectral estimation. The use of frequency decomposition partially circumvents this problem, since in every subband the noise is approximately white. When colored noise is added in the input signal with the individual process in the subbands, it

can be assumed to be white. Nevertheless, the same assumption could not be made in the fullband. That is extremely useful for this case, where the statistics of the input signal not only are not known a priori, but also have to be estimated in space and determined adaptively.

2. SNR Reduction

In order to be able to visualize the SNR reduction that is accomplished with the filter bank decomposition, a number M of sinusoids buried in complex noise $n(n)$ is assumed. Then the signal model $x(n)$ becomes

$$x(n) = \sum_{i=0}^{M-1} A_i e^{j\omega_i n} + n(n), \quad A_i = |A_i| e^{j\phi_i} \tag{1.18}$$

where the amplitudes A_k are unknown but constant with uniformly distributed phase angles in the $[-\pi,\pi)$. For the noise, it is assumed to be a zero mean wide sense stationary (WSS) random process uncorrelated with the sinusoids.

Under the assumption that M is large enough, then $x(n)$ is a zero mean WSS process with the following autocorrelation function [Tcacenko].

$$R_{xx}(k) = \sum_{i=0}^{M-1} P_i e^{j\omega_i k} + R_{nn}(k), \quad P_i = |A_i|^2 \tag{1.19}$$

If the local signal-to-noise ratio is defined for each of the M sinusoids with respect to the noise as SNR_i, then

$$SNR_i = \frac{P_i}{R_{nn}(0)}, \; i=0,\ldots,M-1 \tag{1.20}$$

To keep the model simple ideal filters are assumed. Therefore,

$$R_{x_m x_m}(k) = \sum_{\omega_i \in I_m} M P_i e^{jM\omega_i k} + R_{nn}(k), \quad I_m = \left[\frac{2\pi m}{M}, \frac{2\pi(m+1)}{M} \right) \tag{1.21}$$

where I_m is the band covered by the m^{th} filter. Combining the above Equations 1.19, 1.20, 1.21, one gets

$$SNR_{i,sub} = M(SNR_{i,full}) \tag{1.22}$$

which illustrates that for each of the i sinusoids, the signal-to-noise ratios of the m^{th} subband is greater than the equivalent one in the whole band by a factor of M, inversely

proportional to the bandwidth of each filter. From that, it is easy to see that the estimation in the subbands is going to be more accurate than in the fullband.

At this point, it needs to be mentioned that increasing the decimation of the whole band to a large number *M*, in practice, is not always as profitable as one might think. The reason is that the length of the data in each subband will be

$$\left[\frac{N_s + N_f - 2}{M}\right] + 1 \tag{1.23}$$

where N_s is the number of available observations of the signal *x(n)* and N_f is the length of each of the analysis filters. From here, it can be seen that the brute force approach of increasing the length of each subband would result in the increase of filter length and equitably to the increase of complexity of the filter bank. As a general rule, it could be said that the most appropriate size for *M* would be as large as possible so there would be enough samples in each subband.

3. The Whitening of Noise in the Subbands

It is assumed that the noise *n(n)* of the signal *x(n)* has a nonconstant power spectral density as in Figure 14, and the magnitude square response of the m^{th} analysis filter is as shown in Figure 15.

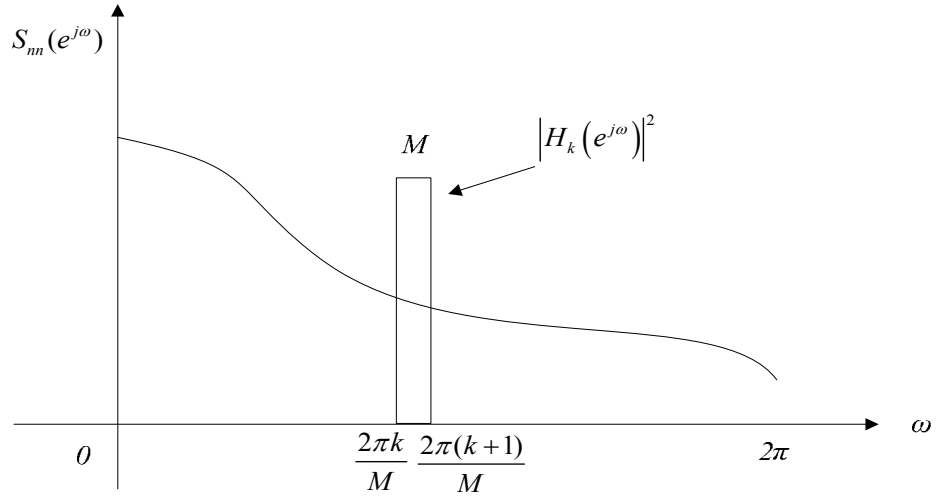

Figure 14. Nonconstant Power Spectral Density [From: Tkacenko]

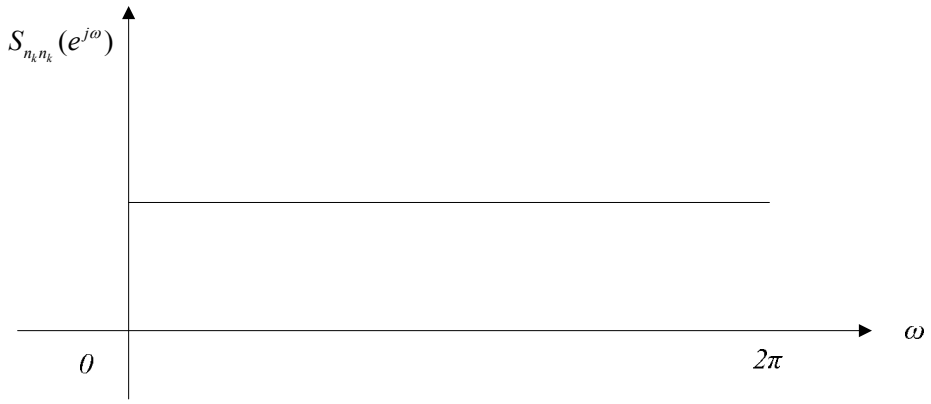

Figure 15. Power Spectrum [From: Tkacenko]

It is very easy to see that while the whole noise spectrum $[0,2\pi]$ is not constant, the smaller area inside the k^{th} subband $\left[\frac{2\pi k}{M}, \frac{2\pi(k+1)}{M}\right]$ is approximately constant. In other words, the larger the selected M is, the smaller the error in the approximation of colored noise with white. However, it should be kept in mind, as mentioned above, that M can not be arbitrarily large.

According to [Tkacenko], with the usage of the spectral flatness measure γ_x^2 of a WSS random process and based on three properties mentioned below, he proves that the weighted geometric mean of the spectral flatness values in the subbands is greater than or equal to the flatness in the fullband. The three properties are that the filter bank is maximally decimated,

$$\sum_{i=0}^{M-1} \frac{1}{n_i} = 1 \tag{1.24}$$

that the magnitude squared response of the i^{th} filter is Nyquist(n_i),

$$\left[\left|H_i\left(e^{j\omega}\right)\right|^2\right]_{\downarrow n_i} = 1 \quad \forall i \tag{1.25}$$

and that the set of analyses satisfies a generalized version of the power complementary property,

$$\sum_{i=0}^{M-1} \frac{\left|H_i\left(e^{j\omega}\right)\right|^2}{n_i} = 1 \quad \forall \omega \tag{1.26}$$

The review of the whole analysis exceeds the objective of this thesis and will not be covered here. [Tkacenko]

F. SUMMARY

As shown in the background theory and literature review, filter banks can be very effective in the estimation of frequencies of sinusoids buried in noise. In particular, when proper filter classes are used for the implementation of the FB, the SNR in the subbands exceeds that in the fullband. In between these classes are the QMF and the FIR filters which the author chose to test here. For both of them, it will be shown how the introduced colored noise affects their behavior and therefore the measurements.

THIS PAGE INTENTIONALLY LEFT BLANK

II. SIGNAL DECOMPOSITION BY FILTER BANKS

In this chapter a general review of the models used in the decomposition of the signal using filter banks is presented. In the first approach, Quadrature Mirror Filters filters were used and in the second approach, DFT FB. Each case was implemented in Matlab's Simulink and the results were compared in terms of accurate frequency estimation.

A. FLEXIBLE STRUCTURE SPACE MODEL

The signal used is generated by the plant presented in [Cristi], modeling the behavior of a flexible structure space model. The main parts are the rigid body and the flexible appendages. The rigid body is modeled as a double integrator ($1/s^2$) and the flexible appendages as a parallel system with underdamped poles. A proportional integral derivative (PID) controller is also implemented in a closed loop to track an external signal, a combination of a step function and a sine wave. The filter bank decomposition the author implemented is added to the output and input signals. The described model as used by the author in Matlab's Simulink, can be seen below in Figure 16. Also in Figure 17 the model's rotation angle in degrees can be seen.

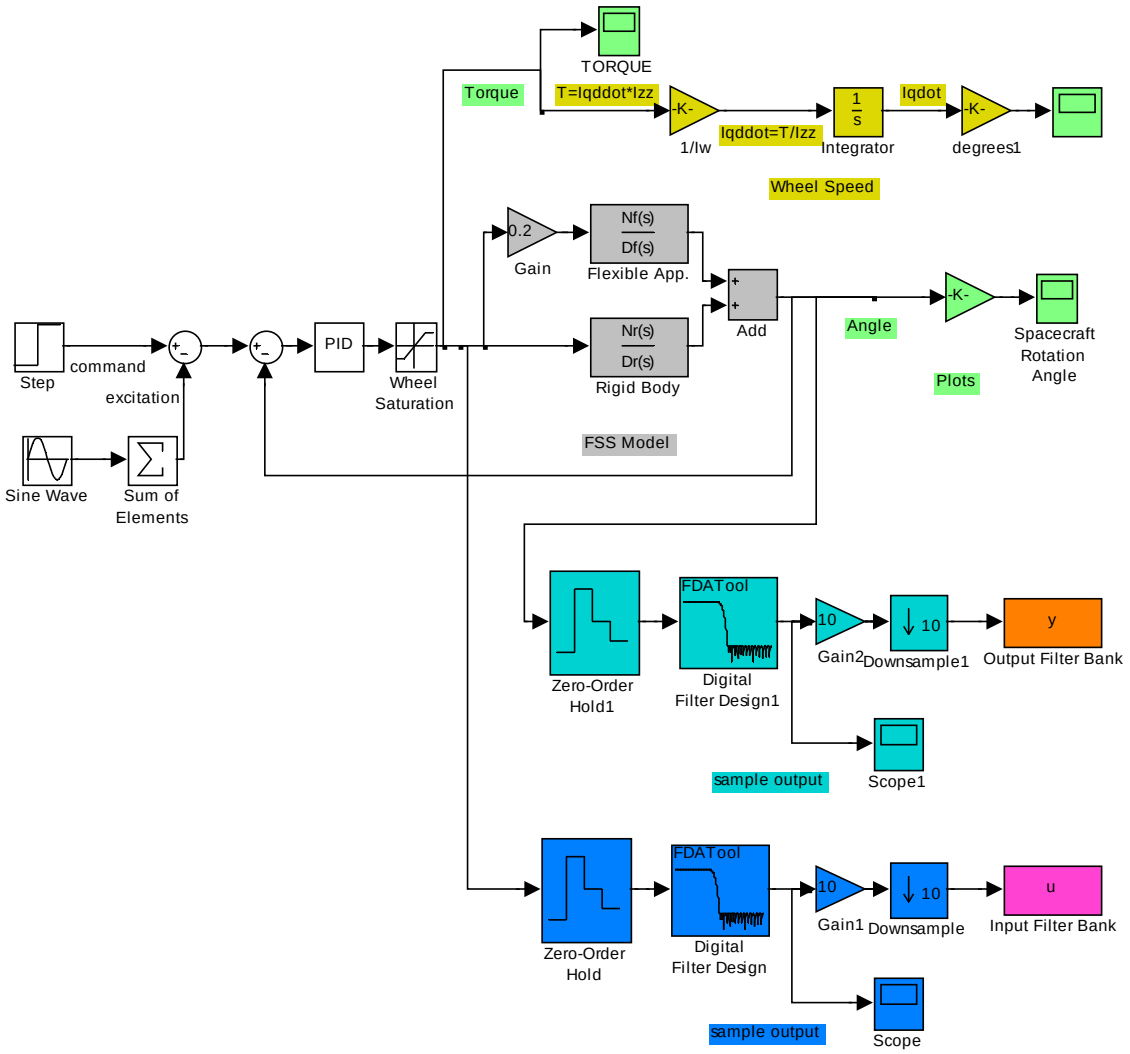

Figure 16. Flexible Structure Space Model

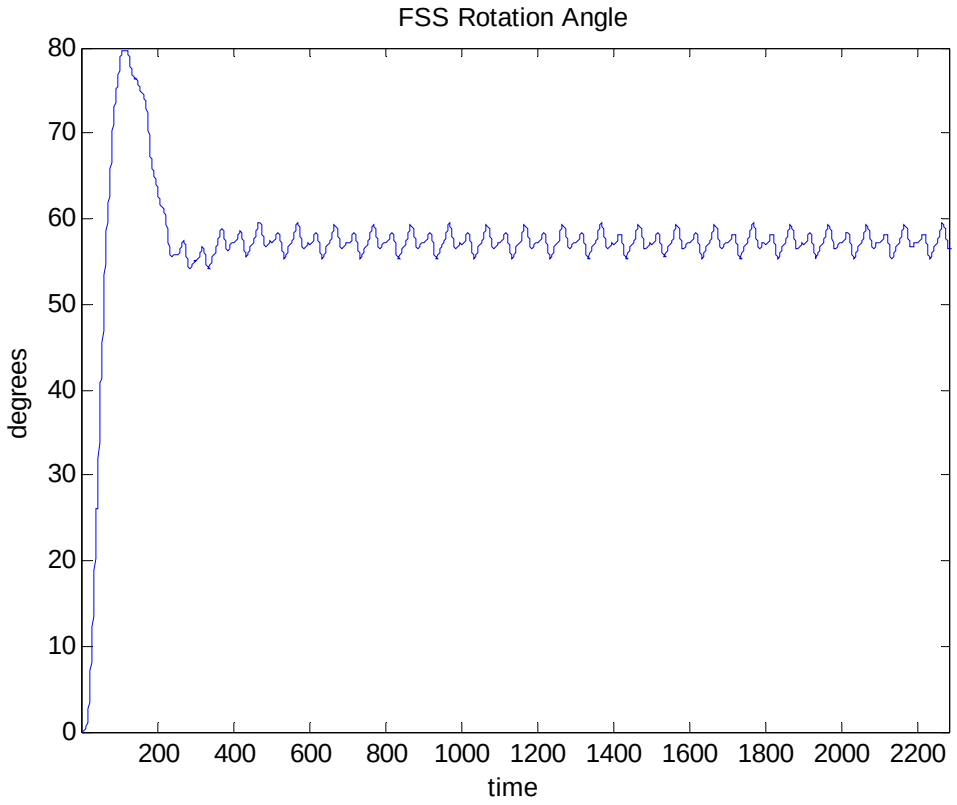

Figure 17. FSS Rotation Angle

Figure 18 shows the output (y) of the model and Figure 19 illustrates the input (u). In both cases, the peak in the beginning from the step function and the ongoing flexibilities can be seen. The filter bank decomposition designed in both cases of the Quadrature Mirror Filters and the DFT FB is going to be applied only to the output (y), but could also be implemented for the input (u) as well.

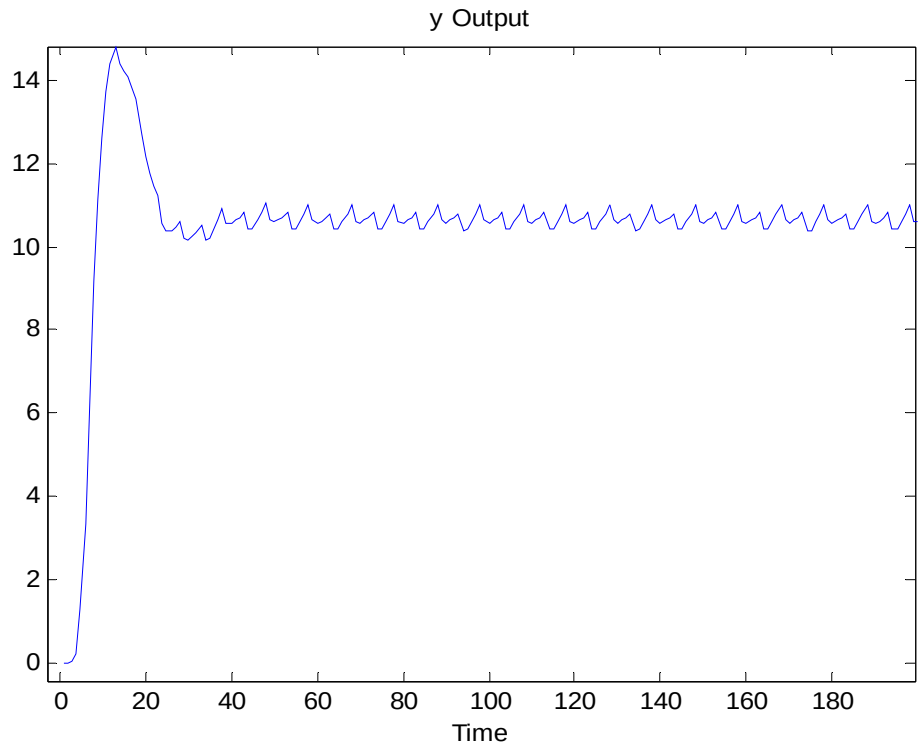

Figure 18. "y" Output from FFS model

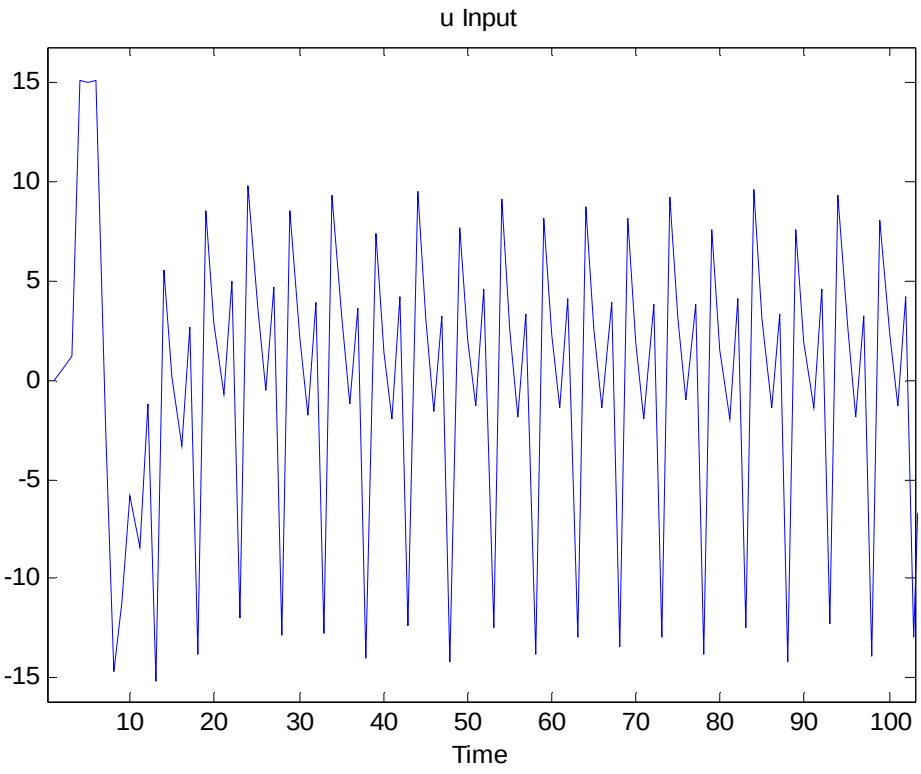

Figure 19. "u" Input to FSS model

B. ANALYSIS WITH QUADRATURE MIRROR FILTERS

As mentioned above, the frequency components of the vibrations were estimated by decomposing the observed signals into a number of channels. In this section the author uses QMF decomposition.

1. Analysis with Quadrature Mirror Filters without Colored Noise

The decomposition is based on the following shown in Figure 20.

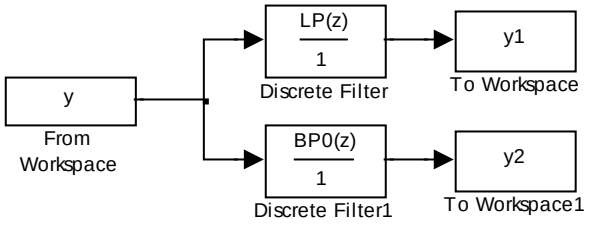

Figure 20. Filter Bank for Two QMFs in Matlab

The signal y coming from the workspace is the output (y) from the FSS model, as a sampled sequence $y[n]=y(nT_s)$ with $T_s=1/F_s$ as the sampling interval. The *LP(z)* and *BP0(z)* filters represent the lowpass filter (*LPF*) and the highpass filter (*HPF*) in Figure 21 respectively. The two bandlimited outputs y_1 and y_2 are maximally decimated by a factor of two in Matlab to give the two corresponding components $y_1[m_1]$ and $y_2[m_2]$ shown in Figure 21 with the same data rate as the original signal.

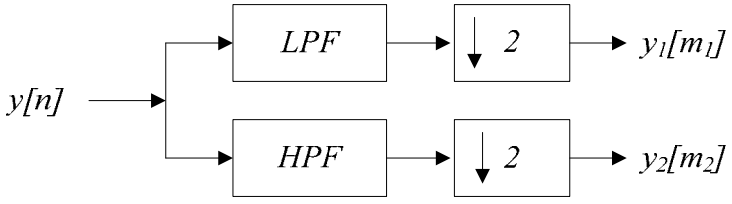

Figure 21. General Model Filter Bank for Two QMFs [After: Cristi]

The two components are sampled at a rate $F_s/2$ and the lowpass and highpass components of the frequency spectrum between zero and $F_s/2$ are mapped as shown in Figure 22. From these two bands, their energy is calculated by taking the standard deviation of the output. For the band that has the bigger energy, the choice is made to decompose it again as before. By following the same procedure, the signal is decomposed into six levels and seven outputs are received from which one can calculate which one has finally the higher energy. The decomposition followed for the FFS model output is shown in Figure 23.

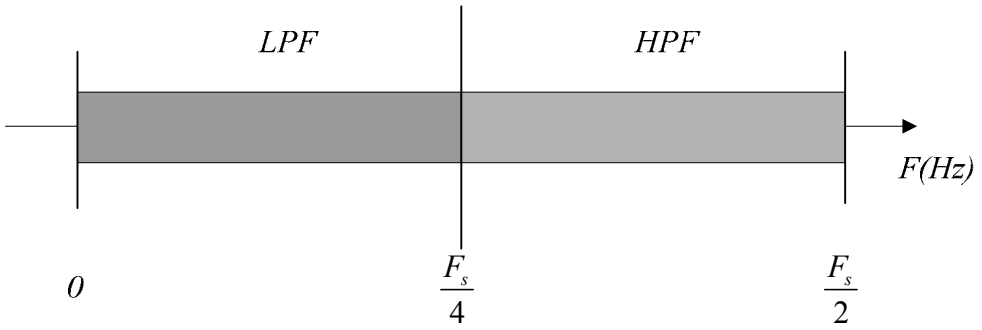

Figure 22. Frequency Bands for Two QMFs [After: Cristi]

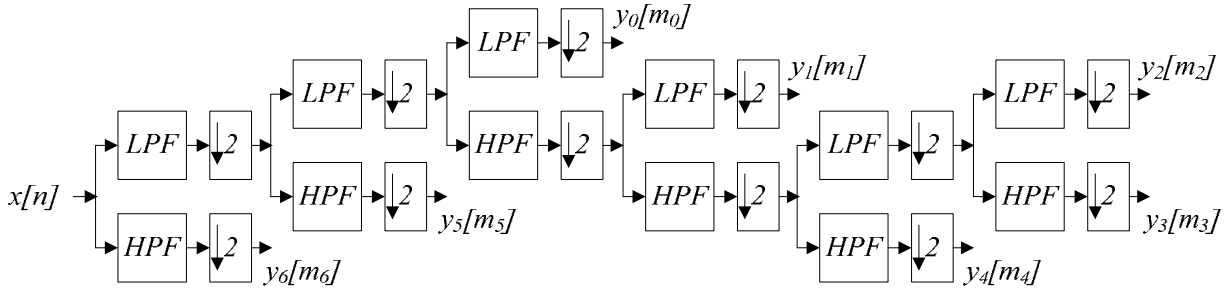

Figure 23. Frequency Decomposition Using Cascaded Filters

Even though the higher energy for the given signal is always going to be in the LP band because of the step function used in the FSS model, it is chosen to modify the decomposition after the third layer to the HP band. The reason is to estimate the dominant

frequency by the higher energy, which is still lower than the energy of the step function. For the same reason, the output content of the lower frequency component caused by the step function, is discarded.

Based on the Noble Identity shown below in Figure24 [Cristi], the author finally has the filter bank shown in Figure 25 with the frequency decomposition displayed in Figure 26.

Figure 24. Noble Identity [From: Cristi]

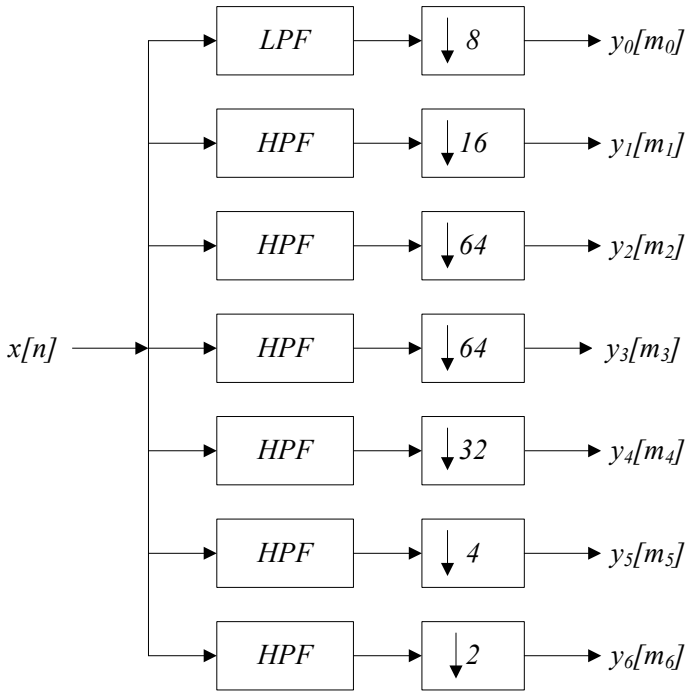

Figure 25. Filter Bank for Eight QMFs

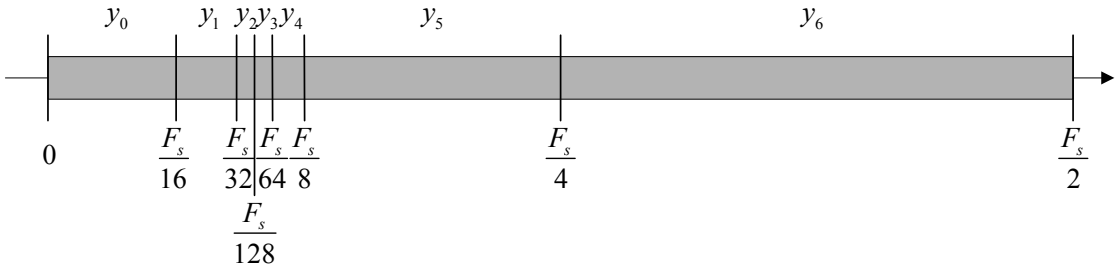

Figure 26. Frequency Bands for Eight QMFs

The above decomposition, as implemented in Matlab, is also shown in Figure 27, where if *g(z)* is the first LP filter and *h(z)* is the first HP filter, then the following transfer functions are obtained: $LP(z) = g(z)g(z^2)g(z^4)$, $BP0(z) = g(z)g(z^2)h(z^4)g(z^8)$, $BP1(z) = g(z)g(z^2)h(z^4)h(z^8)g(z^{16})g(z^{32})$, $BP2(z) = g(z)g(z^2)h(z^4)h(z^8)g(z^{16})h(z^{32})$, $BP3(z) = g(z)g(z^2)h(z^4)h(z^8)h(z^{16})$, and $BP4(z) = g(z)h(z^2)$ and $LP(z) = h(z)$.

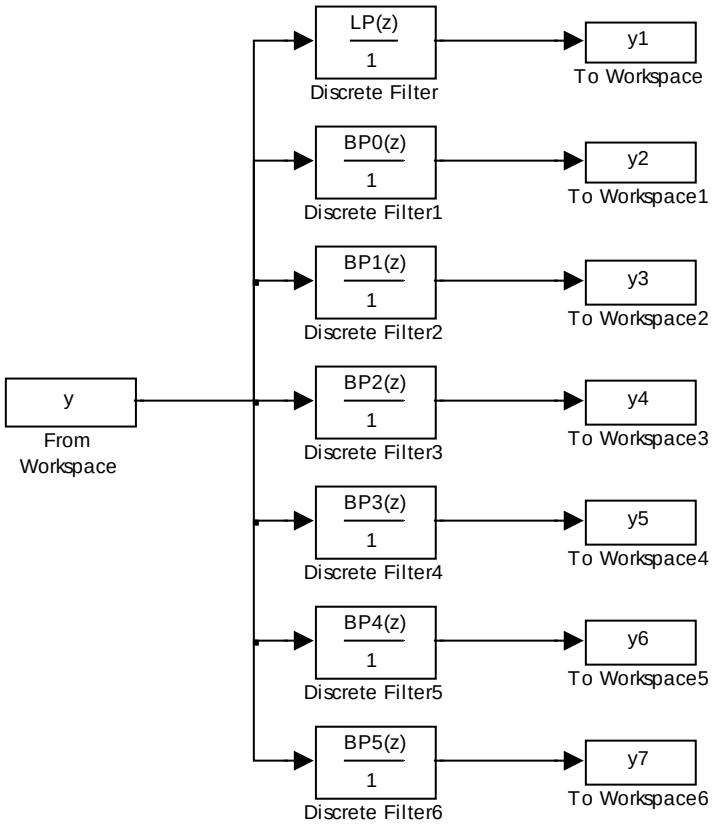

Figure 27. Filter Bank with QMF in Matlab

For F_s=*1Hz* the following two pairs of graphs (Figures 28 and 29) with tables (Tables 1 and 2) are obtained that show the energies within different frequency ranges. The first pair shows the energy of the outputs for dB15 and the second one for dB45. The rest of the graphs and tables for two, three, four, five, six, and again seven outputs for the case of dB15 are shown in Appendix A. At this point it needs to be mentioned that the whole analysis the author followed was based on the outcomes of the dB15 case and would have had a different filter bank analysis if the analysis was based on the dB45 case.

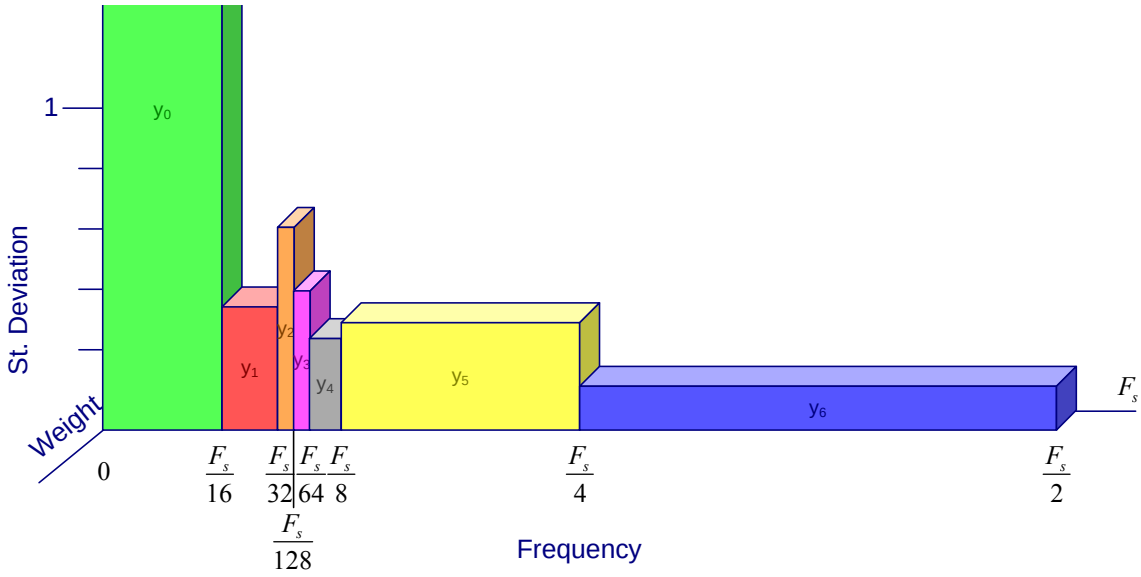

Figure 28. Standard Deviation of Seven QMD filters for dB15

Standard Deviation of Seven QMF Filters for dB15							
Output	**y_0**	**y_1**	**y_2**	**y_3**	**Y_4**	**y_5**	**y_6**
Standard Deviation	7.2592	0.3434	0.6996	0.3848	0.2636	0.2747	0.1019

Table 1. Standard Deviation of Seven QMF filters for dB15

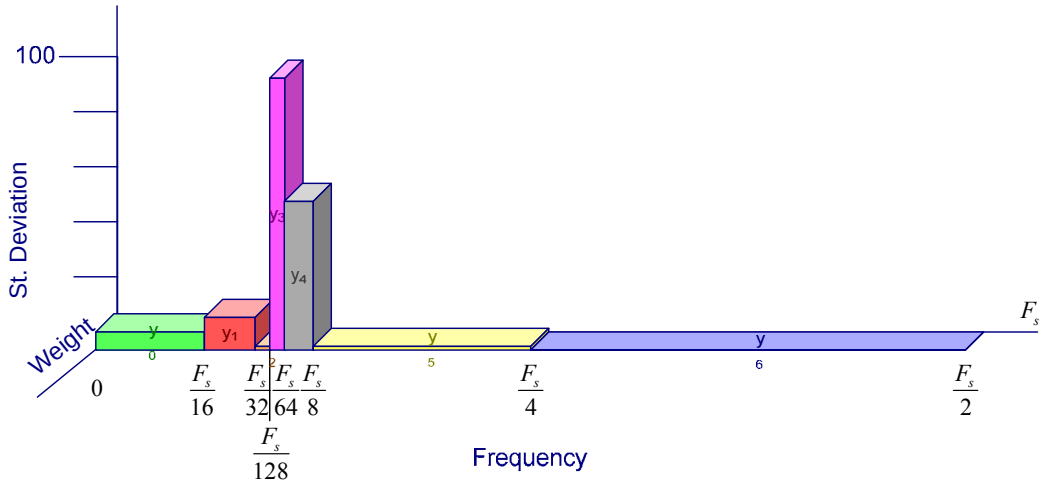

Figure 29. Standard Deviation of Seven QMF filters for dB45

Standard Deviation of Seven QMF filters for dB45							
Output	**y_0**	**y_1**	**y_2**	**y_3**	**Y_4**	**y_5**	**y_6**
Standard Deviation	12.4913	20.1186	0.2717	94.5267	49.9890	2.3487	0.1494

Table 2. Standard Deviation of Seven QMF filters for dB45

Based on this decomposition, the spectral components with the highest energy are known and the frequency response of the system within this frequency band can be estimated. Below in Figure 30 and Table 3 the wanted frequency subband with the higher energy is isolated with the use of weights.

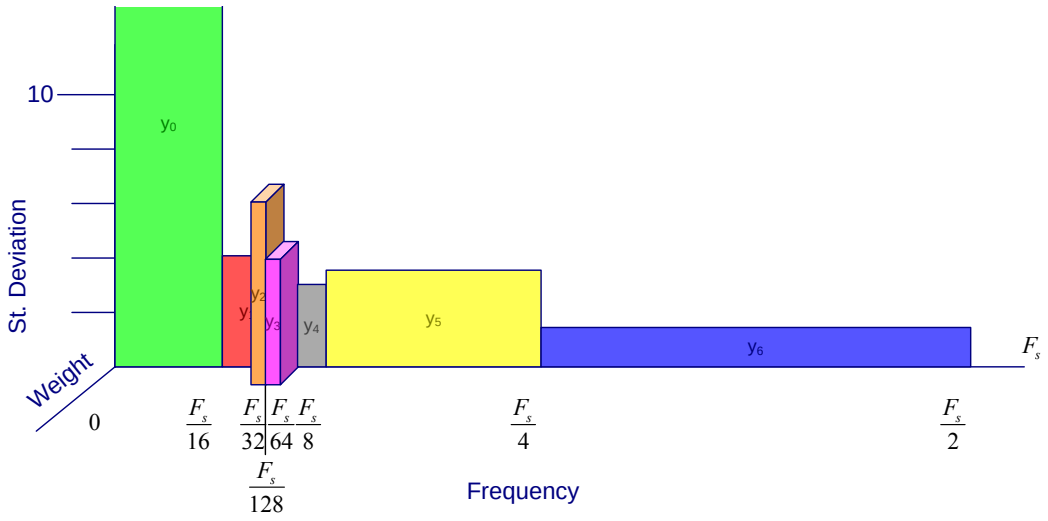

Figure 30. Standard Deviation of Seven Weighted QMF Filters for dB15

Standard Deviation of Seven weighted QMF filters for dB15							
Output	**y_0**	**y_1**	**y_2**	**y_3**	**y_4**	**y_5**	**y_6**
Standard Deviation	0	0	0.6996	0.3848	0	0	0

Table 3. Standard Deviation of Seven Weighted QMF Filters for dB15

Furthermore, in order for the system to be adaptive and dynamic the author developed a system of loops in Matlab that selects each time the higher output of the stage and decomposes it again. The loop was repeated four times and the same five outputs as in the case from the previous model for five outputs should have been obtained. This time though, the selection could not be guided like was the case before where after the third decomposition the author chose not to divide again the higher-in-energy subband coming from the step response in the lowpass area. Here the author lets the system decide for every decomposition and so the higher energy subband is as expected in the lower frequency subband with different values for the graph and table than before. Bellow in Figure 31 is the model used for that dynamic decomposition and after that its outputs in the Tables 4 and 5 for 15 and 45dB, respectively.

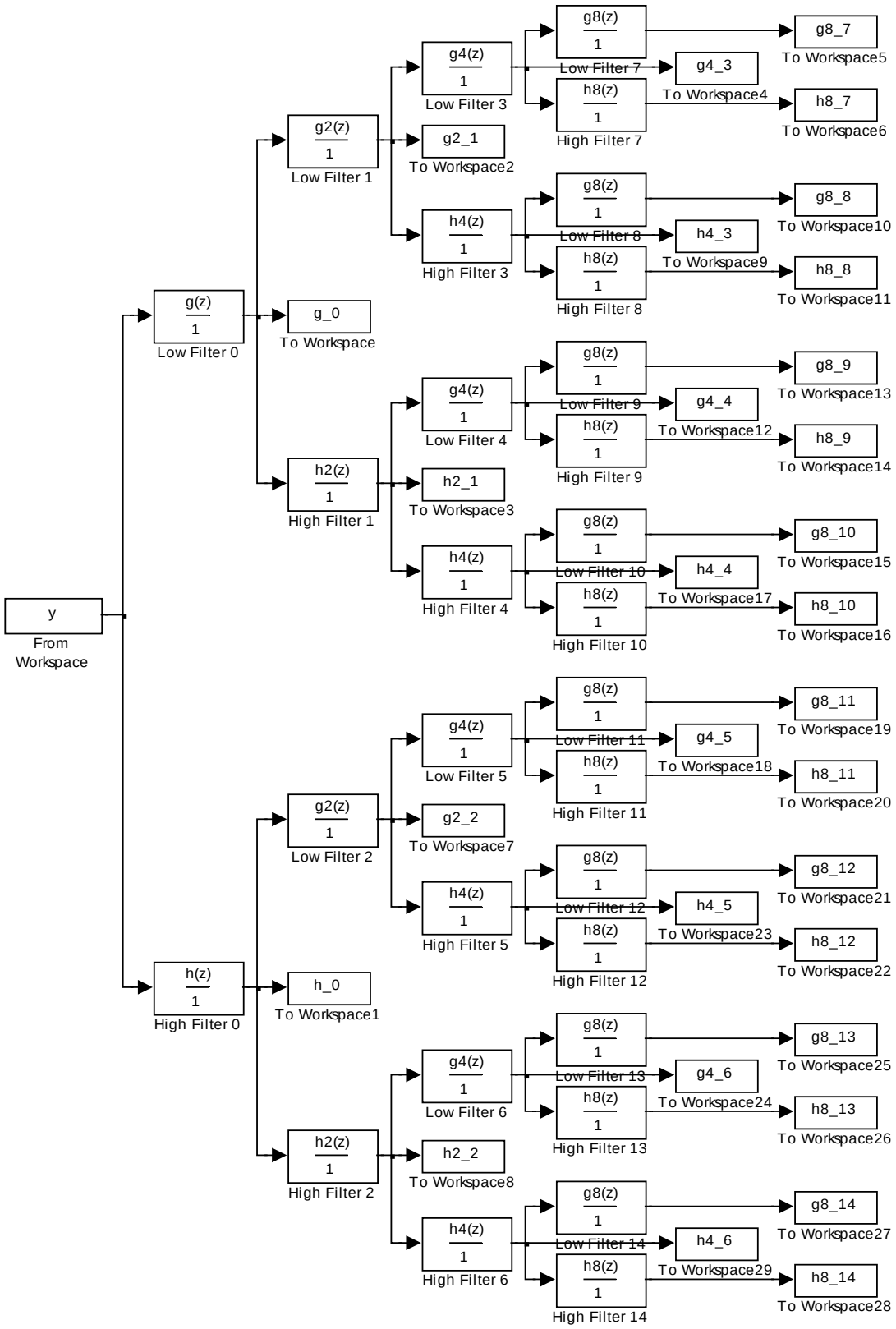

Figure 31. Dynamic Filter Bank of Four stages

Standard Deviation of Dynamic Bank with Five QMF Filters for dB15					
Output	y_0	y_1	y_2	y_3	y_4
Standard Deviation	14.3204	1.1609	0.3977	0.2747	0.1019

Table 4. Standard Deviation of Dynamic Bank with Five QMF Filters for dB15

Standard Deviation of Dynamic Bank with Five Filters for dB45					
Output	y_0	y_1	y_2	Y_3	y_4
Standard Deviation	22.8628	17.3112	4.8914	2.3487	0.1494

Table 5. Standard Deviation of Dynamic Bank with Five QMF Filters for dB45

Even though in both cases of dB15 and dB45 the higher-in-energy output can be clearly selected each time, in the second case the numbers are more accurate because of the higher order Daubechies filter. Finally here, weights can be used again to isolate the outputs that are preferred.

2. Analysis with Quadrature Mirror Filters with Colored Noise

For the author to be able to fully see the advantages of the above decomposition, colored noise is added to the model as shown below in Figure 32, with the power spectrum shown in Figure 33.

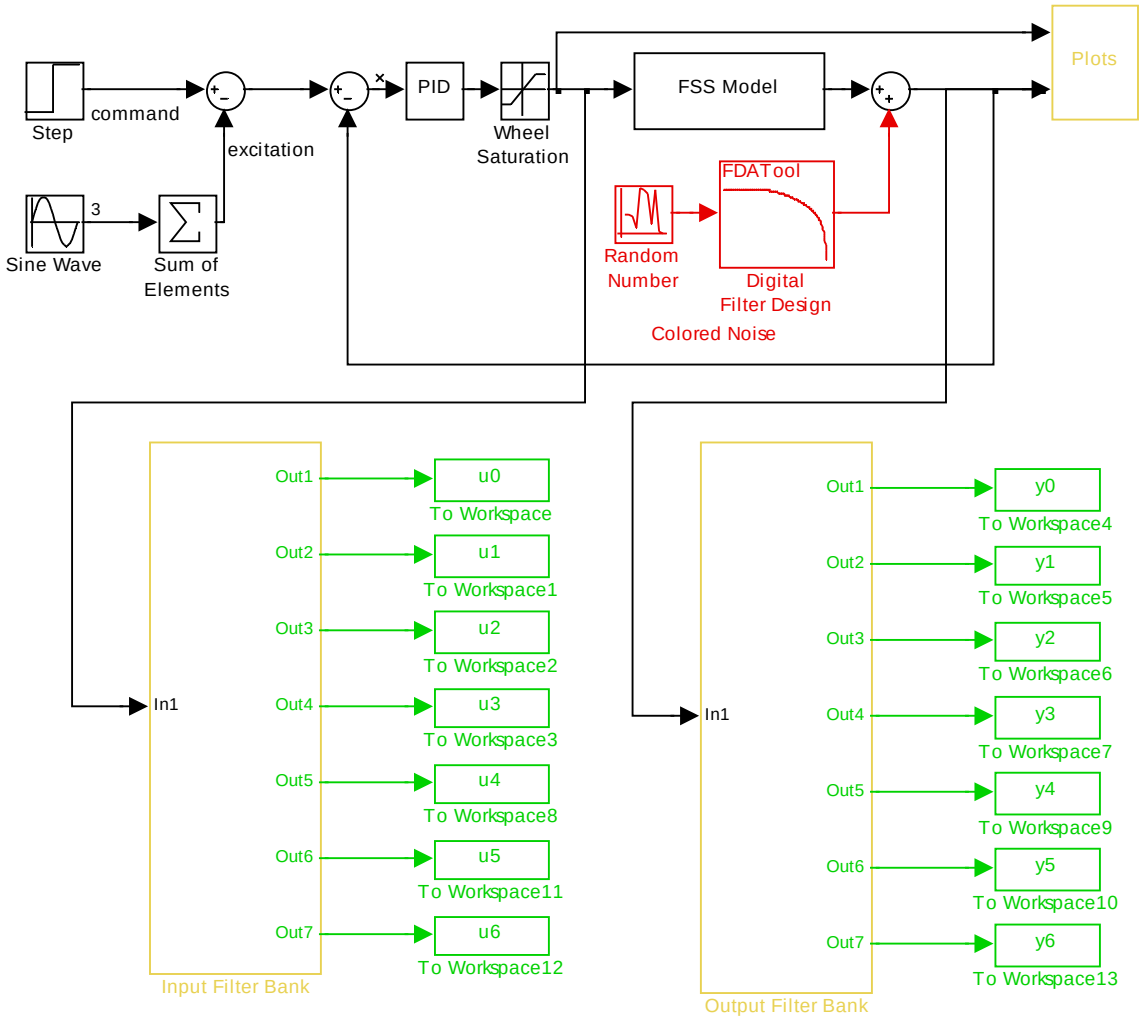

Figure 32. FSS Model with Colored Noise for the QMF

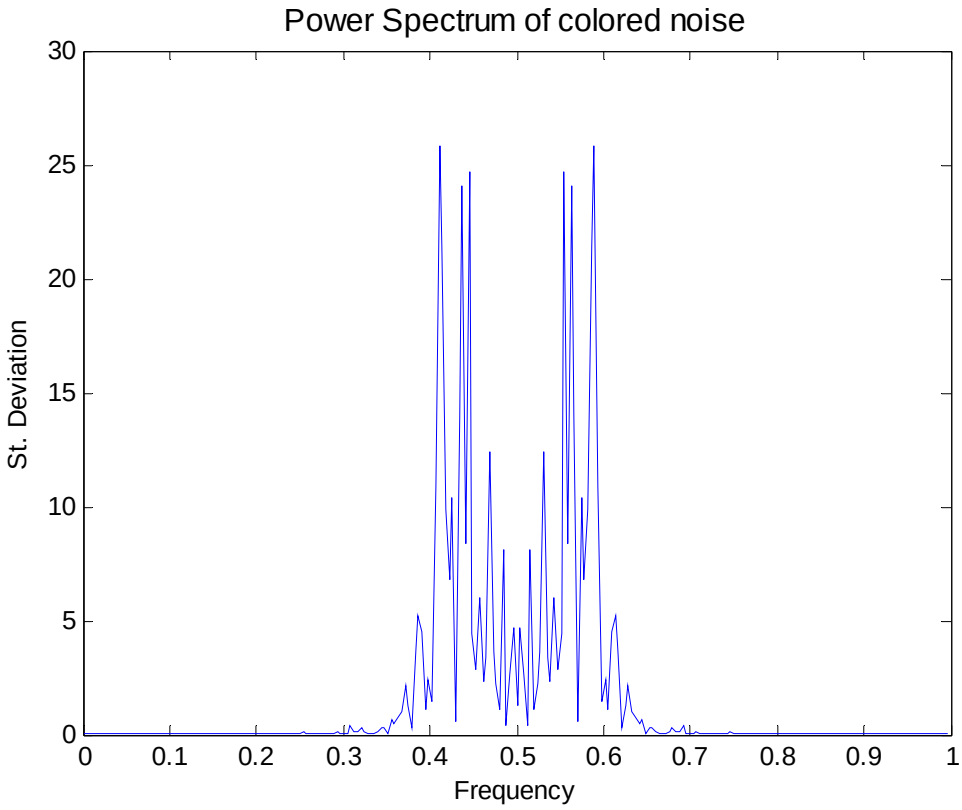

Figure 33. Power Spectrum of the Used Colored Noise

After the added colored noise, the standard deviations of the new outputs are again calculated and the author gets the graphs in Figures 34 and 35 and tables in Tables 6 and 7. From these values, the author can clearly say that the added noise did not affect the model since the values are analogous to the previous ones when the model had no added noise. The rest of the graphs and tables for two, three, four, five, six and again seven outputs for the case of dB15 with added colored noise are shown in Appendix B.

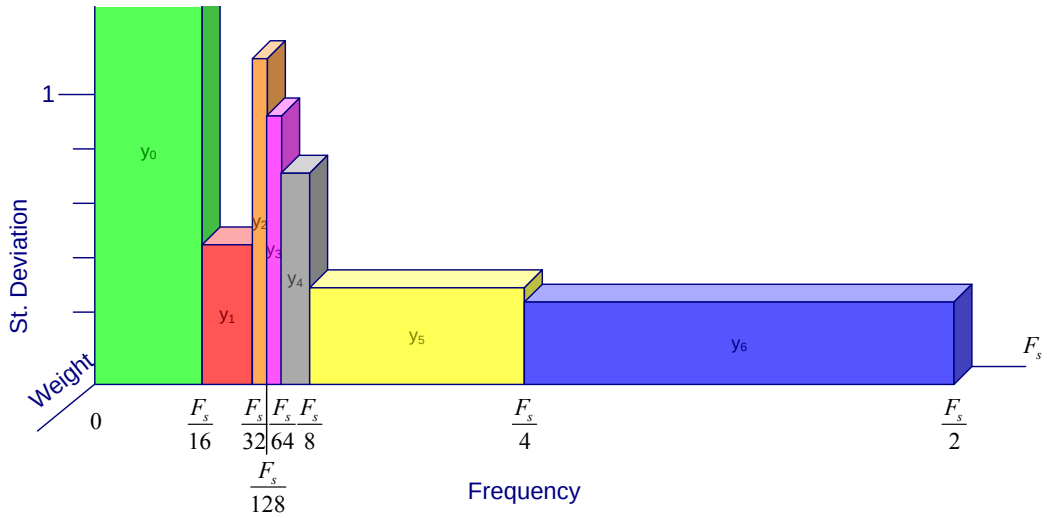

Figure 34. Power Spectrum with Colored Noise of Seven QMF Filters for dB15

Standard Deviation with Colored Noise of Seven QMF Filters for dB15							
Output	**y_0**	**y_1**	**y_2**	**y_3**	**y_4**	**y_5**	**y_6**
Standard Deviation	408370	0.4769	1.1954	0.9899	0.7239	0.3727	0.3545

Table 6. Standard Deviation with Colored Noise of Seven QMF Filters for dB15

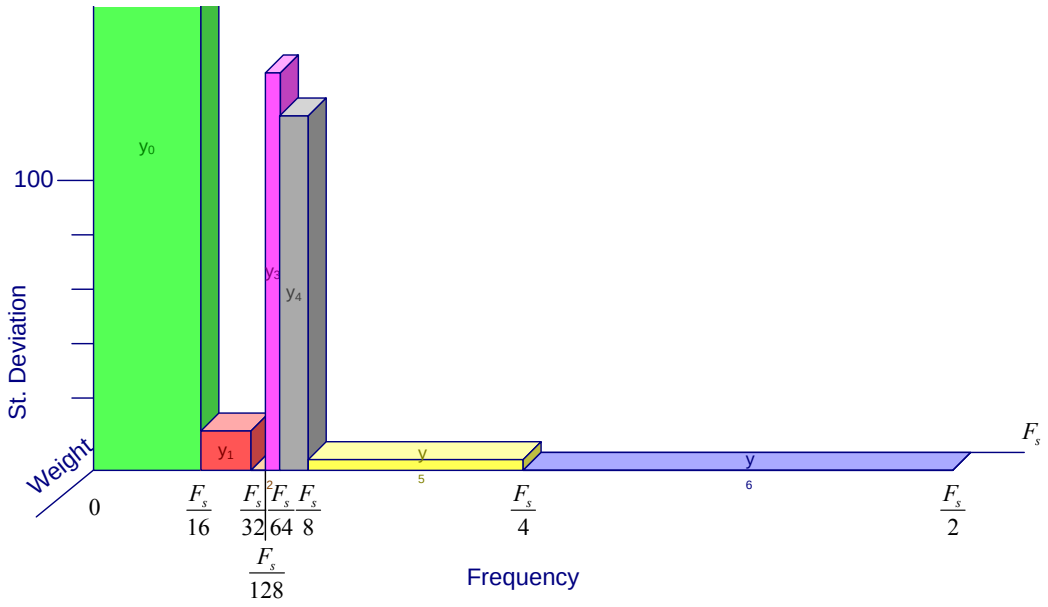

Figure 35. Standard Deviation with Colored Noise of Seven QMF Filters for dB45

Standard Deviation with Colored Noise of Seven QMF Filters for dB45							
Output	y_0	y_1	y_2	y_3	y_4	y_5	y_6
Standard Deviation	250980	17.8080	0.0321	144.6512	133.0226	3.7517	1.0448

Table 7. Standard Deviation with Colored Noise of Seven QMF Filters for dB45

Analogous results are gotten if the same colored noise is applied to the dynamic FB for five outputs (Tables 8 and 9).

Standard Deviation with Colored Noise of Dynamic Bank with Five Filters for dB15					
Output	y_0	y_1	y_2	y_3	Y_4
Standard Deviation	409440	5.8021	0. 7592	0. 3727	0. 3545

Table 8. Standard Deviation with Colored Noise of Dynamic Bank with Five QMF Filters for dB15

Standard Deviation with Colored Noise of Dynamic Bank with Five Filters for dB45					
Output	y_0	y_1	y_2	y_3	Y_4
Standard Deviation	322720	80.2683	10.5877	3.7517	1.0448

Table 9. Standard Deviation with Colored Noise of Dynamic Bank with Five QMF Filters for dB45

C. ANALYSIS WITH DFT FILTER BANKS

Another class of filters that preserves the energy of a signal when it is being decomposed into subbands is the FIR filters, while satisfying the conditions described in the background theory. Even though the author was not able to use ideal filters because of

their infinite order, an approximation was made via the use of a FIR filter with order 63 as the original filter. Likewise, the order can very easily be increased for more accurate results, which goes beyond the purpose of this thesis. Below are the block parameters of the original filter used in Matlab.

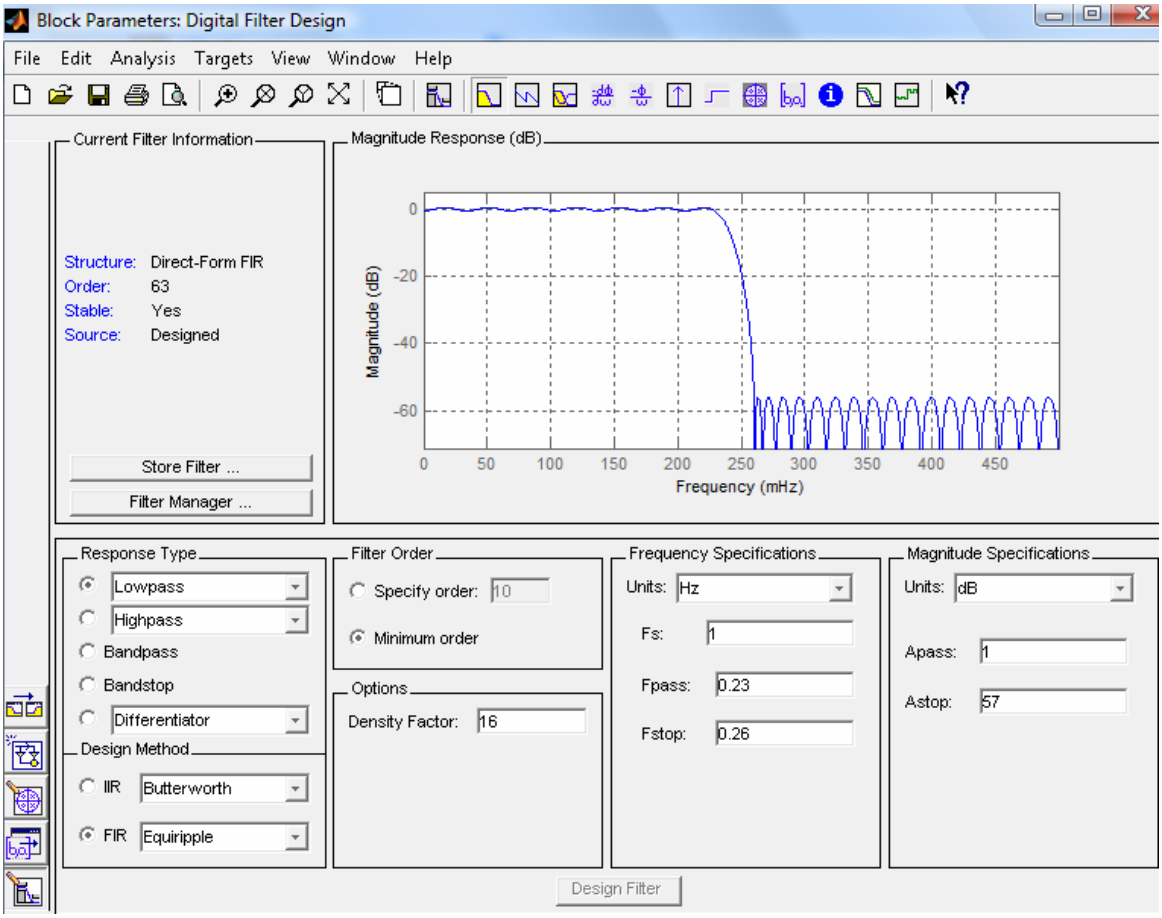

Figure 36. Block Parameters of the Used FIR Filter

1. Analysis with FIR Filters without Colored Noise

For the analysis with the above filter, a filter bank was created using the polyphase components in Matlab as shown in Figure 37. Each one of the new filters has 64/8 coefficients from the original FIR filter and processes the signal with a delay of z^{-1} from the previous one. From that filter bank comes eight outputs, of which IFFT as described in the background theory is taken. Then, the standard deviation is calculated in each channel. From the values obtained, the determination is made as to which subband

has the higher energy. These results can be seen in Figure 38 along with Table 10. Again, as in the QMF case, there is a high value in the lower frequencies because of the step function which is disregarded.

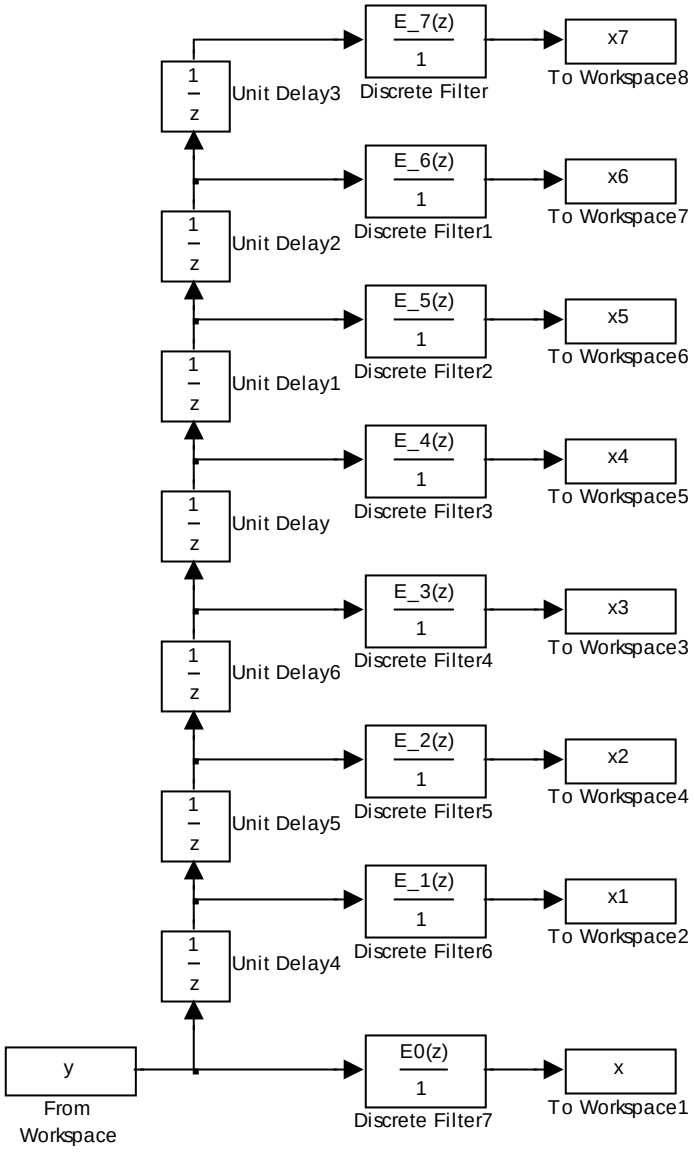

Figure 37. Filter Bank with Eight FIR Filters

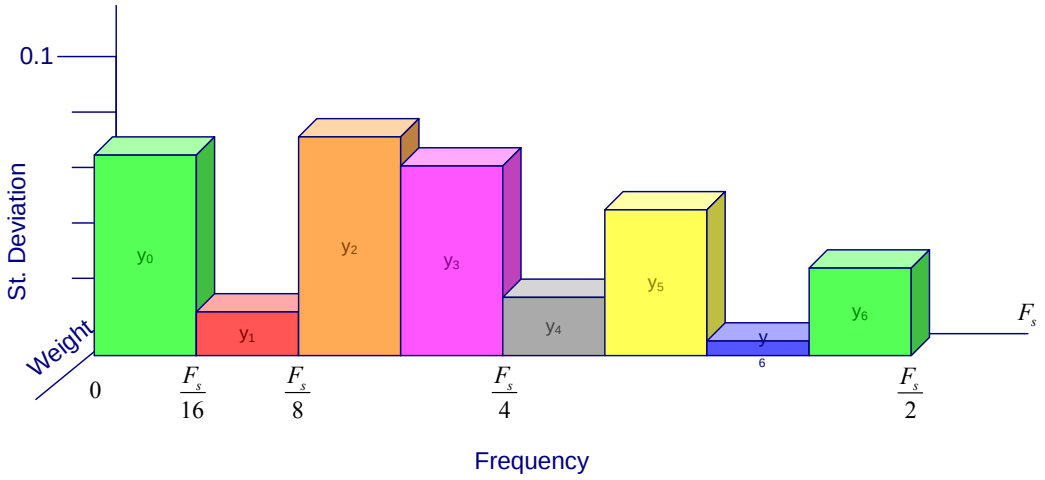

Figure 38. Standard Deviation of Eight FIR filters

Standard Deviation of Eight FIR filters								
Output	**Y_0**	**y_1**	**y_2**	**y_3**	**y_4**	**y_5**	**y_6**	**y_7**
Standard Deviation	0.0727	0.0171	0.0766	0.0704	0.0249	0.0507	0.0072	0.037

Table 10. Standard Deviation of Eight FIR filters

2. Analysis with FIR Filters with Colored Noise

On the above model the same colored noise used in Section III.B.2 for the QMF case was added. The results for the colored signal can be seen below in Figure 39 and Table 11. If these results are compared with the previous ones, namely the case without the colored noise, it will again be verified that they are analogous. It is obvious that no matter the added colored noise, the filter bank was able to distinguish again, with high precision, the higher-in-energy subbands.

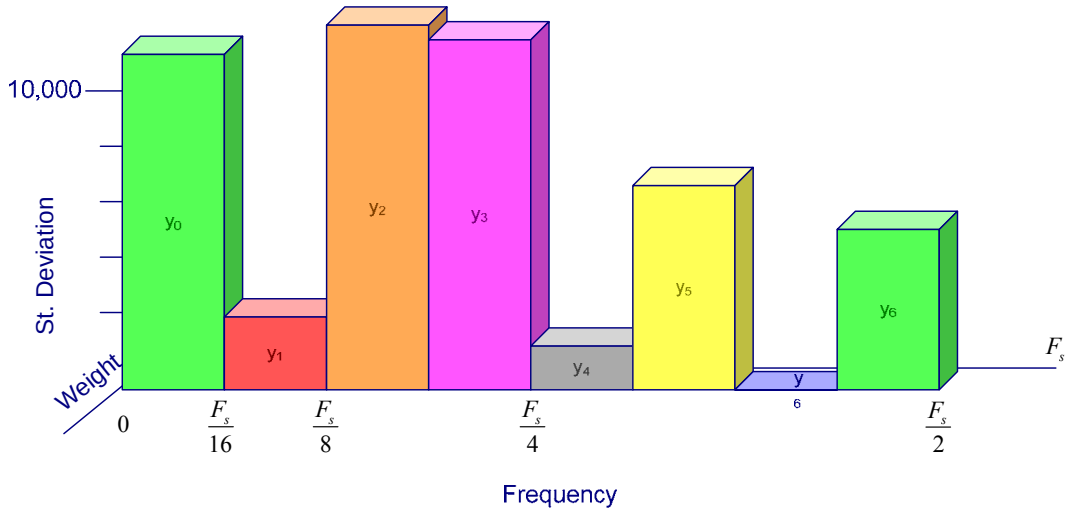

Figure 39. Standard Deviation of Eight FIR Filters with Colored Noise

Standard Deviation of Eight FIR Filters with Colored Noise								
Output	**y_0**	**y_1**	**Y_2**	**y_3**	**y_4**	**y_5**	**y_6**	**y_7**
Standard Deviation	11383.3	1911.3	12699.0	11888.2	1406.7	7267.1	6.4108	5499.1

Table 11. Standard Deviation of Eight FIR Filters with Colored Noise

D. SUMMARY

In this chapter, the behavior of FB implemented with QMF and FIR filters was examined. For each case the author applied a signal initially noise-free and then with added colored noise. The measurements taken were presented in tables and bar charts for easier comparison. All the findings and deductions are summarized in Chapter III.

THIS PAGE INTENTIONALLY LEFT BLANK

III. CONCLUSIONS

In this thesis a method of frequency estimation by Quadrature Mirror Filters and Filter Banks was introduced. They both provide a suitable decomposition of the signal in terms of the various frequency components.

Both approaches are very efficient in terms of the number of operations. The particular advantage is that they provide an estimate of the frequencies within a specified interval.

Indeed, the results in both cases satisfy the theoretical expectations. For the first case with the QMF it was seen that while decomposing the original signal the results are leading towards the same subband. Analogous values were received even in the case with the dynamic FB for five outputs with the mentioned difference due to the altered decomposition algorithm. Likewise, for the second case with the FIR filters the standard deviation in all the subbands increased when the colored noise was added, but still in an analogous fashion.

If these two decomposition Filter Banks are compared, it can be seen that the QMF for the same number of outputs gives a more accurate result, meaning that the determined subband is a lot narrower. Moreover, as the level of decomposition is extended, the difference between them also grows.

On the other hand, the case of QMF has the disadvantage of having to calculate the energy of each subband on each level of the decomposition. That procedure introduces a number of serious calculations which results in an increase of the system's feedback time. For the calculating procedure used in this thesis, the FB with the FIR filters gave the faster results either with or without the colored noise.

As a final conclusion it could be said that both cases have their positive and negative sides, so the selection should be made each time depending on the environment and requirements of the current application.

Further processing, although not addressed in this thesis, is to refine the estimates by properly modeling the system and estimating the parameters. In this case the two

proposed approaches have the advantage that they use the signal only in a narrow part of the spectrum, thus yielding a better signal-to-noise ratio and better “whiteness” of the noise spectrum. Further research needs to be undertaken to develop this method.

APPENDIX A: GRAPHS AND TABLES OF THE QMF FILTER BANK FOR DB15

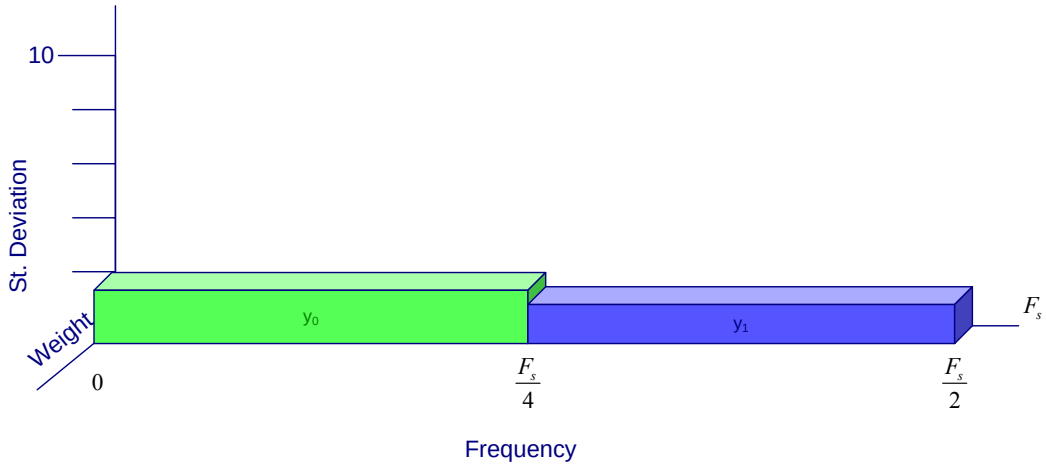

Figure 40. Standard Deviation of Two QMF Filters for dB15

Standard Deviation of Two QMF Filters for dB15		
Output	**y_0**	**y_1**
Standard Deviation	1.5630	0.1019

Table 12. Standard Deviation of Two QMF Filters for dB15

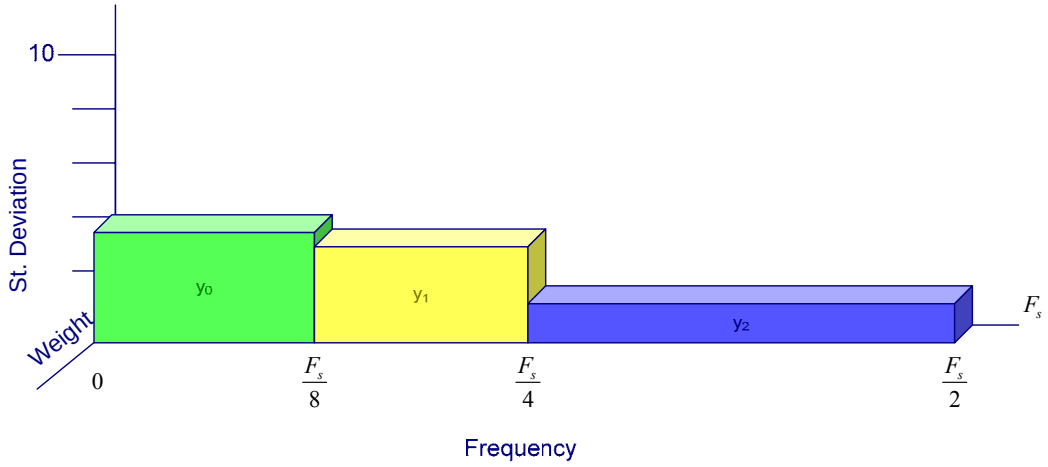

Figure 41. Standard Deviation of Three QMF Filters for dB15

Standard Deviation of Three QMF Filters for dB15			
Output	**y_0**	**y_1**	**y_2**
Standard Deviation	3.5030	0.2747	0.1019

Table 13. Standard Deviation of Three QMF Filters for dB15

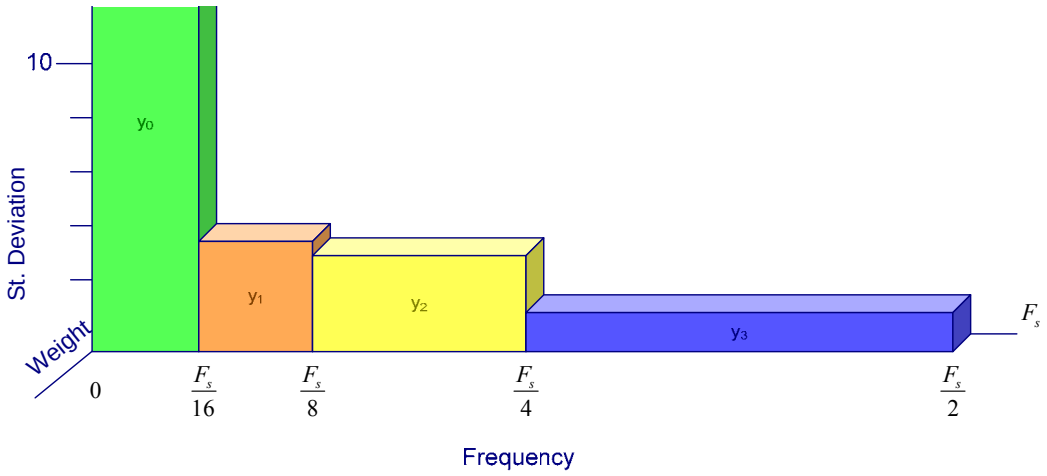

Figure 42. Standard Deviation of Four QMF Filters for dB15

Standard Deviation of Four QMF Filters for dB15				
Output	**y_0**	**y_1**	**y_2**	**y_3**
Standard Deviation	7.2592	0.3977	0.2747	0.1019

Table 14. Standard Deviation of Four QMF Filters for dB15

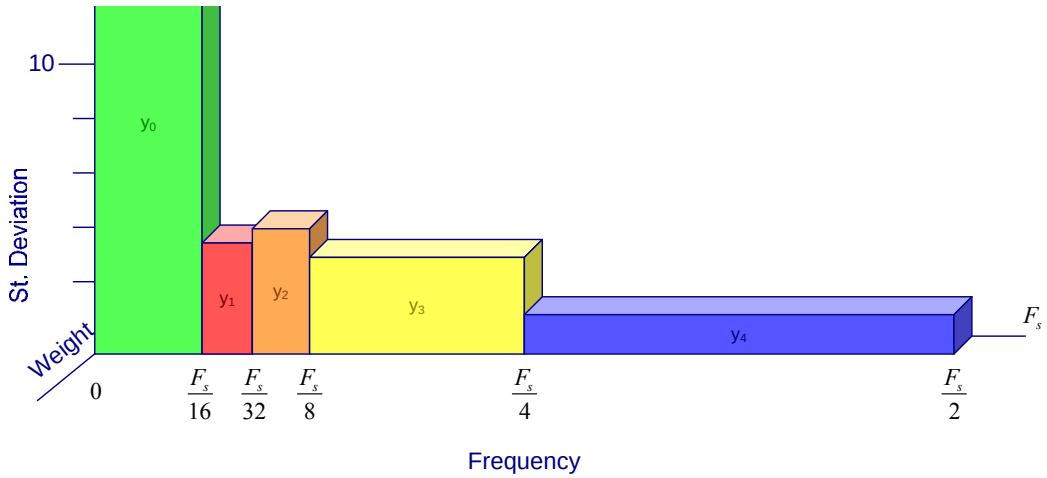

Figure 43. Standard Deviation of Five QMF Filters for dB15

Standard Deviation of Five QMF Filters for dB15					
Output	**y_0**	**y_1**	**Y_2**	**y_3**	**y_4**
Standard Deviation	7.2592	0.3434	0.4345	0.2747	0.1019

Table 15. Standard Deviation of Five QMF Filters for dB15

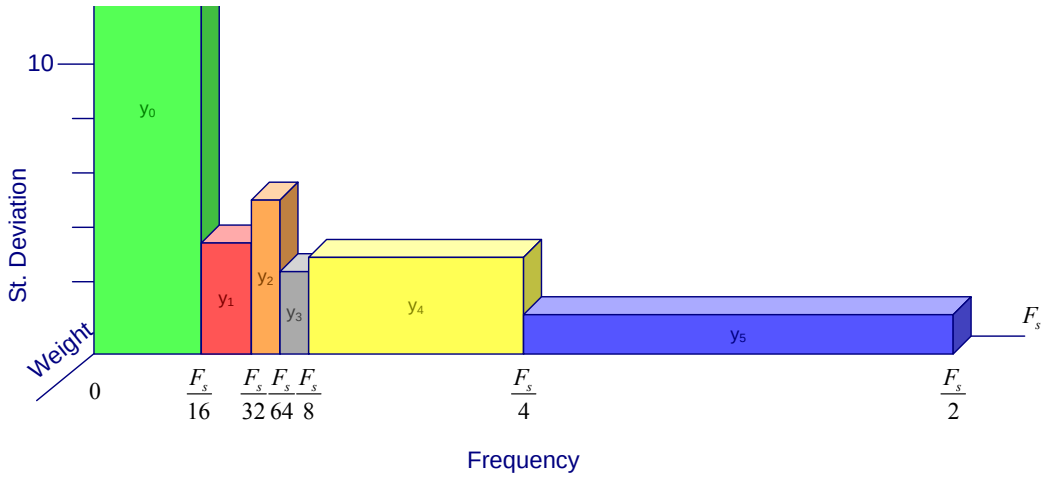

Figure 44. Standard Deviation of Six QMF Filters for dB15

Standard Deviation of Six Filters for dB15						
Output	**y_0**	**y_1**	**y_2**	**y_3**	**y_4**	**y_5**
Standard Deviation	7.2592	0.3434	0.5587	0.2636	0.2747	0.1019

Table 16. Standard Deviation of Six QMF Filters for dB15

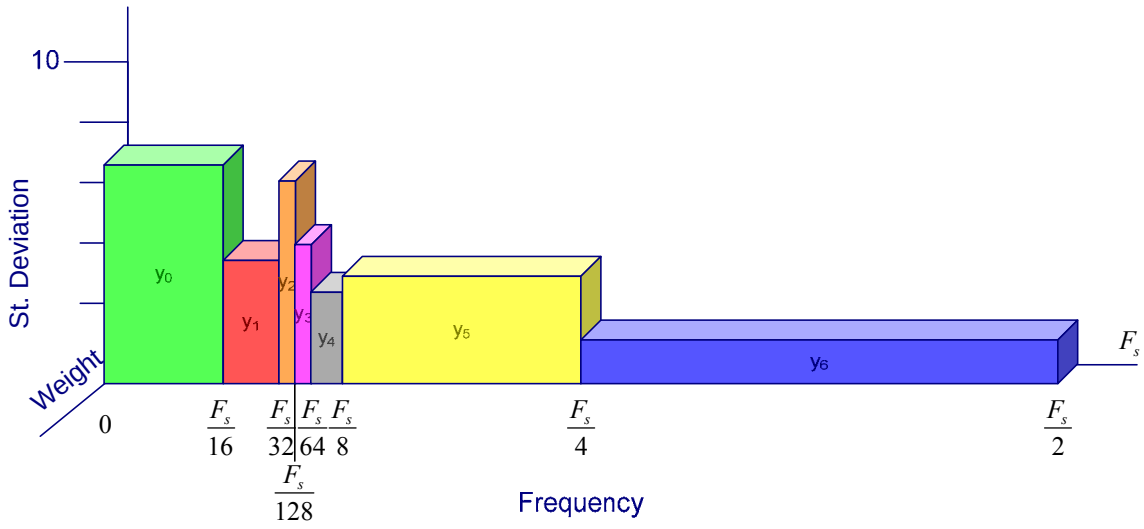

Figure 45. Standard Deviation of Seven QMF Filters for dB15

Standard Deviation of Seven QMF Filters for dB15							
Output	**y_0**	**y_1**	**y_2**	**y_3**	**y_4**	**y_5**	**y_6**
Standard Deviation	7.2592	0.3434	0.6996	0.3848	0.2636	0.2747	0.1019

Table 17. Standard Deviation of Seven QMF Filters for dB15

APPENDIX B: GRAPHS AND TABLES OF THE QMF FILTER BANK FOR DB15 WITH ADDED COLORED NOISE

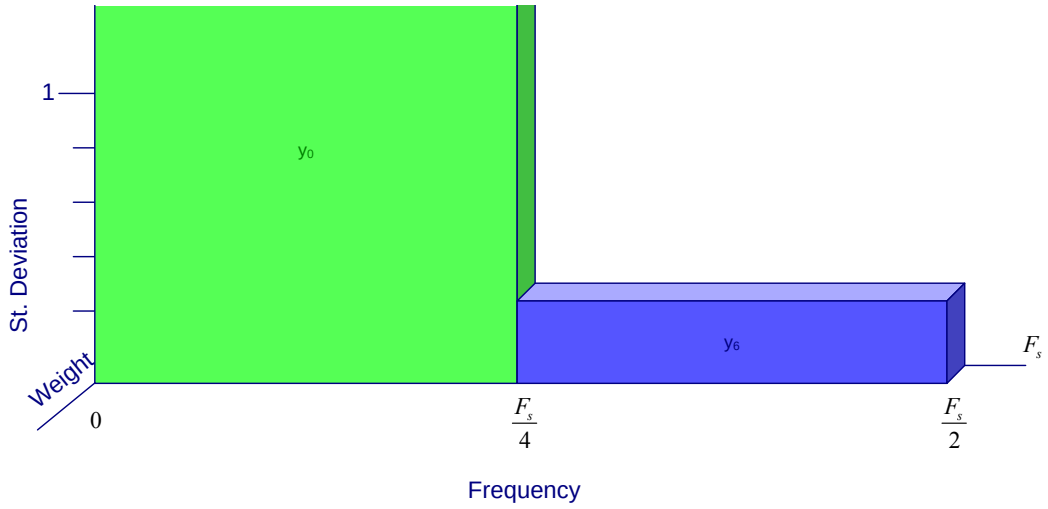

Figure 46. Standard Deviation of Two QMF Filters for dB15 with Added Colored Noise

Standard Deviation of Two QMF Filters for dB15 with Added Colored Noise		
Output	**y_0**	**y_1**
Standard Deviation	274910	0.3545

Table 18. Standard Deviation of Two QMF filters for dB15 with Added Colored Noise

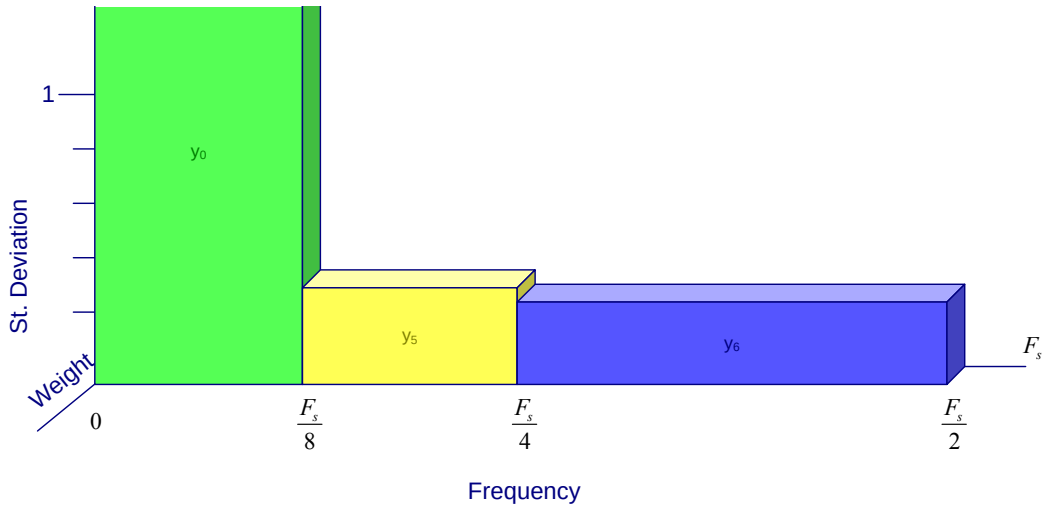

Figure 47. Standard Deviation of Three QMF Filters for dB15 with Added Colored Noise

Standard Deviation of Three QMF Filters for dB15 with Added Colored Noise			
Output	**y_0**	**y_1**	**y_2**
Standard Deviation	351440	0. 3727	0.3545

Table 19. Standard Deviation of Three QMF Filters for dB15 with Added Colored Noise

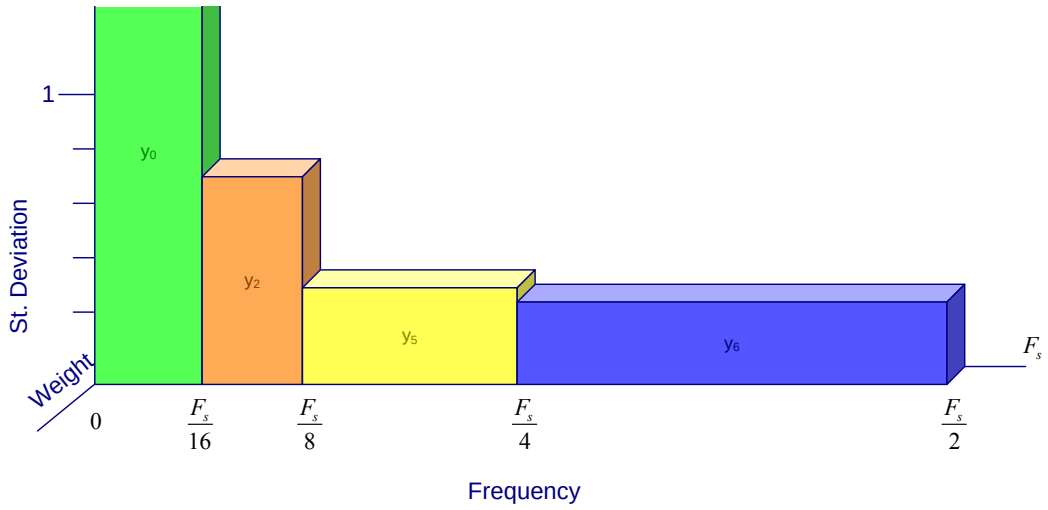

Figure 48. Standard Deviation of Four QMF filters for dB15 with Added Colored Noise

Standard Deviation of Four QMF Filters for dB15 with Added Colored Noise				
Output	**y_0**	**y_1**	**y_2**	**y_3**
Standard Deviation	408370	0. 7592	0. 3727	0.3545

Table 20. Standard Deviation of Four QMF Filters for dB15 with Added Colored Noise

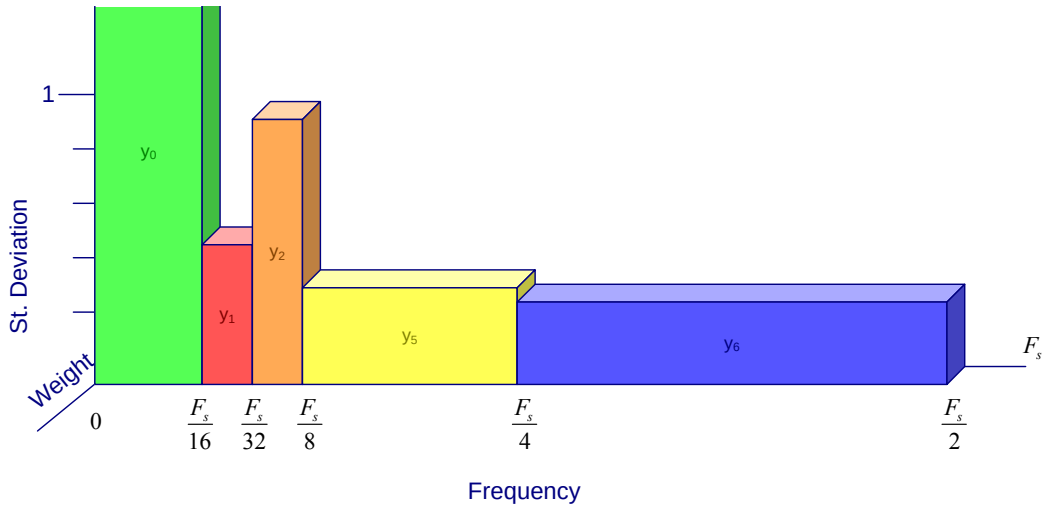

Figure 49. Standard Deviation of Five QMF Filters for dB15 with Added Colored Noise

Standard Deviation of Five QMF filters for dB15 with Added Colored Noise					
Output	**y_0**	**y_1**	**y_2**	**y_3**	**y_4**
Standard Deviation	408370	0. 4769	0. 9357	0. 3727	0.3545

Table 21. Standard Deviation of Five QMF Filters for dB15 with Added Colored Noise

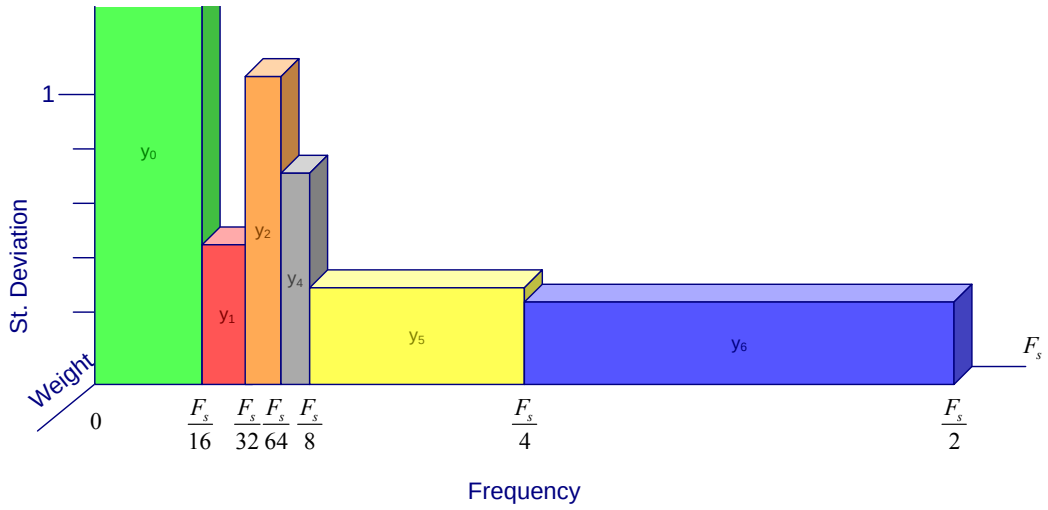

Figure 50. Standard Deviation of Six QMF Filters for dB15 with Added Colored Noise

Standard Deviation of six Filters for dB15 with Added Colored Noise						
Output	**y_0**	**y_1**	**y_2**	**y_3**	**y_4**	**y_5**
Standard Deviation	408370	0. 4769	1.1053	0. 7239	0. 3727	0.3545

Table 22. Standard Deviation of Six QMF Filters for dB15 with Added Colored Noise

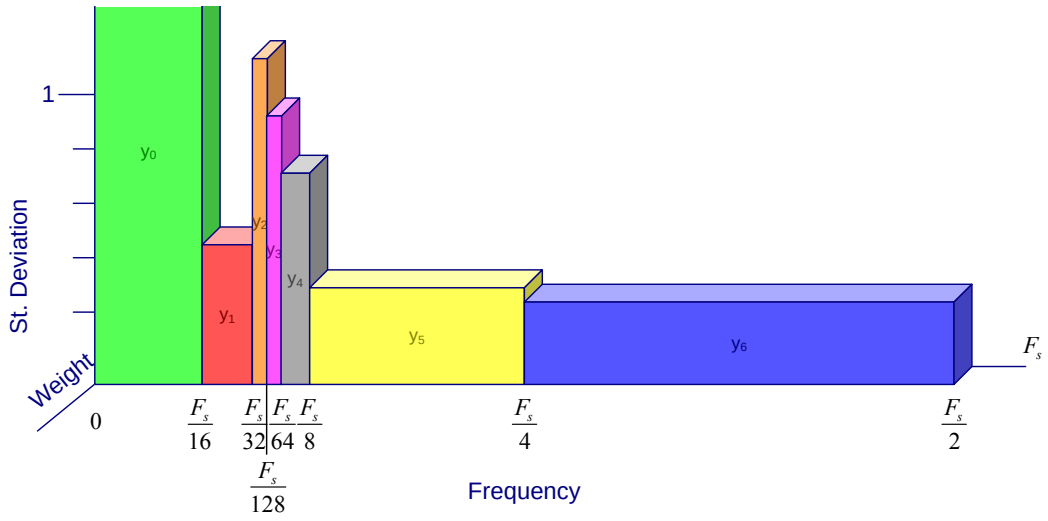

Figure 51. Standard Deviation of Seven QMF Filters for dB15 with Added Colored Noise

Standard Deviation of Seven QMF Filters for dB15 with Added Colored Noise							
Output	**y_0**	**y_1**	**y_2**	**y_3**	**y_4**	**y_5**	**y_6**
Standard Deviation	408370	0.4769	1.1954	0.9899	0.7239	0.3727	0.3545

Table 23. Standard Deviation of Seven QMF Filters for dB15 with Added Colored Noise

LIST OF REFERENCES

[Cristi] R. Cristi, *Control of flexible Structures: Frequency Estimation*, Unpublished Report, Department of Electrical and Computer Engineering, Naval Postgraduate School, Monterey, California, September 2006.

[Cristi1] R. Cristi, *Modern Digital Signal Processing*, 1st edition, Thomson Brooks/Cole, Pacific Grove, California, 2004.

[Galand] Claude R. Galand and Henri J. Nussbaumer "New Quadrature Mirror Filter Structures," IEEE Transactions on Acoustics, Speech, and Signal Processing, Vol. ASSP-32, No. 3, June 1984.

[Jain] Vijay K. Jain and Ronald E. Crochiere, "Quadrature Mirror Filter Design in the Time Domain," IEEE Transactions on Acoustics, Speech, and Signal Processing, Vol. ASSP-32, No. 2, April 1984.

[Karapatakis] K. Karapatakis, Adaptive Control Of A Laser Tracking Device For Space Based Application, Master's Thesis, Naval Postgraduate School,, Monterey, California, September 2006.

[Lin] Yuan-Pei Lin and P.P. Vaidyanathan, "A Kaiser Window Approach for the Design of Prototype Filters of Cosine Modulated Filter Banks," IEEE Signal Processing Letters, Vol. 5, No. 6, June 1998.

[Losada] Ricardo A. Losada, "Practical FIR Filter Design in MATLAB," Revision 1.1, The MathWorks, Inc., 3Apple Hill Dr. Natick, MA 01760, USA, January 2004.

[Manos] E. Manos, Control of a System in the Presence of Flexible Modes, Master's Thesis, Expected Completion June 2007.

[Sandrock] Malte Sandrock and Stefan Schmitt, "Realization of an Adaptive Algorithm with Subband Filtering Approach for Acoustic Echo Cancellation in Telecommunication Applications," DSPesialists GmbH, D-10245, Germany.

[Swaminathan] Kumar Swaminathan and P. P. Vaidyanathan, "Theory and Design of Uniform DFT, Parallel, Quadrature Mirror Filter Banks," IEEE Transactions on Circuits and Systems, Vol. CAS-33, No. 12, December 1986.

[Tkacenko] Andre Tkacenko and P.P. Vaidyanathan, "The Role of Filter Banks in sinusoidal Frequency Estimation," California Institute of Technology, 136-93 Moore, Pasadena, California 91125.

[Vaidyanathan] Andre Tkacenko and P.P. Vaidyanathan, "Sinusoidal Frequency Estimation Using Filter Banks," *IEEE Proceedings*, p.p. 3089-3092, 2001.

INITIAL DISTRIBUTION LIST

1. Defense Technical Information Center
   Ft. Belvoir, Virginia

2. Dudley Knox Library
   Naval Postgraduate School
   Monterey, California

3. Chairman, Code EC
   Department of Electrical and Computer Engineering
   Naval Postgraduate School
   Monterey, California

4. Roberto Cristi
   Department of Electrical and Computer Engineering
   Naval Postgraduate School
   Monterey, California

5. Xiaoping Yun
   Department of Electrical and Computer Engineering
   Naval Postgraduate School
   Monterey, California

6. Konstantinos Tzellos
   Hellenic Navy
   Athens, Greece